Response to the reviewer's comments for manuscript cp-2017-151

Dear Dr. Beaufort,

We would like to acknowledge the time and effort that you and two anonymous reviewers have invested in order to assess the previous version of our manuscript. Please find below our point-by-point responses to the reviewers' comments and suggestions. We hope that our comments below are sufficiently clear, but please do not hesitate to contact us if there are any problems. In order to simplify the tracing of the improvements made in the main text as a response to the reviewer's suggestions and to further improve readability/clarity, we have highlighted all changes.

We would like to thank you in advance for further consideration of our manuscript for publication in *Climate of the Past*.

On behalf of all co-authors,
Kim Jakob

Response to Reviewer #1

R.1.1: "Thermocline state change in the Eastern Equatorial Pacific during the late Pliocene/early Pleistocene intensification of Northern Hemisphere Glaciation by Jakob et al. This manuscript uses a combination of foraminiferal geochemistry (Mg/Ca and stable oxygen and carbon isotopes), abundance and sand accumulation rate to reconstruct how the thermocline in the east Pacific cold tongue area developed during the onset of Northern Hemisphere Glaciation (2.4–2.75 Ma). The comparison between foram species living at the surface and in the (sub)-thermocline gives an estimate on how deep the thermocline was and, thus, on the intensity of upwelling and primary productivity. The new data in this study are focused on geochemistry of the deep dwelling *G. crassaformis* and abundance of thermocline species. These show a shift around 2.6 Ma when the intermediate dwellers decrease in abundance and the deep-dwelling *G. crassaformis* increases suggesting a switch towards a shallower thermocline afterwards. This may have played a role in the development of larger ice sheets in the Northern Hemisphere. Interestingly, the temperature and $\delta^{18}O$ records do not show this shift but neither a clear glacial-interglacial cyclicity. A longer-term trend seems to be present, although it is unclear what could have caused this.

In general, this manuscript is well-written, concise and easy to read providing new high-resolution data for an area and time interval during which a lot was happening. What I am missing a bit is the interaction with other studies dealing with this theme to come to a clear mechanism what caused what, i.e. a shallow thermocline led to more ice build-up or the other way around?"

We thank the reviewer for this positive assessment. Substantial shoaling of the thermocline as documented by our data from ~2.64 to 2.55 Ma suggests that major changes in thermocline depth occurred shortly before the final phase of the late Pliocene/early Pleistocene intensification of Northern Hemisphere Glaciation (iNHG) and that (sub-)tropical thermocline shoaling, perhaps, was a precondition to allow the development of large ice sheets in the Northern Hemisphere. Our observation is in line with studies from Fedorov et al. (2006) and Dekens et al. (2007), but contradicts the results of Wara et al. (2005), Steph et al. (2006a, 2010) and Ford et al. (2012). The latter have documented most prominent changes in thermocline depth only prior to ~3.5 Ma (see Fig. S2.1 in our Response Letter to Reviewer #2).

A brief discussion on what caused what, i.e., whether thermocline shoaling favoured Northern Hemisphere ice build-up or *vice versa*, as asked by the reviewer, has already been included in the original version of the manuscript (Section 5.4.2, p. 12, lines 6–10). To ac-

count for the reviewer's comment, however, we will elaborate this discussion in more detail, also in comparison with other studies as also suggested by Reviewer #2 (Section 5.4.2, p. 13, lines 3–14)*.

R.1.2: "A lot of work has been done already, both specifically for this time interval, but also for the full Pliocene/Pleistocene showing how long-term trends did develop. And although several studies are mentioned throughout the text as "supporting" the new data, I think the manuscript would improve if the current study is projected for example onto the longer trends and/or compared with model experiments. This would also help to determine if an apparent trend in $\Delta\delta^{18}O$ and ΔMg/Ca fits in with the overall trend, i.e. the thermocline shoaling throughout the east Pacific in Steph et al. (2010) does show a lot of variability occurring around 2.5–2.7 Ma. So could it be that the reconstructions here are more temporal variability than a long-term change?"

We highly appreciate this suggestion. Our new records ($\delta^{18}O$ and Mg/Ca gradients) from Site 849 indicate a general shoaling of the thermocline across the entire target interval (~2.75–2.4 Ma), and therefore can be termed a "long-term" shoaling trend, although the most prominent thermocline shoaling is restricted to the ~2.64–2.55 Ma period (see new Fig. 8). The overall shoaling trend observed at Site 849 across the Plio-Pleistocene transition matches results from previous proxy records and modelling efforts (Wara et al., 2005; Fedorov et al., 2006; Dekens et al., 2007; Steph et al., 2006a, 2010; Ford et al., 2012) that consistently document a "long-term" shoaling of the thermocline in the Eastern Equatorial Pacific (EEP) and other (sub-)tropical upwelling regions throughout the Plio-Pleistocene.

Upon closer inspection, however, the geochemical (Mg/Ca and $\delta^{18}O$) records of the thermocline-dwelling species *G. tumida* from Site 1241 in the East Pacific Warm Pool reveal a short-term, i.e., "transient" thermocline deepening from ~2.7 to 2.5 Ma that is superimposed on the overall "long-term" shoaling trend observed in this study for ~6–2 Ma (Steph et al., 2006a, 2010; see new Fig. 8, see also Fig. S2.1 in our Response Letter to Reviewer #2).

"Transient" thermocline deepening from ~2.7 to 2.5 Ma as shown for Site 1241 (Steph et al., 2006, 2010) contradicts our proxy records for thermocline depth at Site 849 that rather indicate a "long-term" thermocline shoaling trend for this time interval; unfortunately, other records used to infer thermocline evolution in the tropical east Pacific for this interval lack the required temporal resolution (i.e., ~12.5 kyr [Site 847; Wara et al., 2005], ~10–20 kyr

* Sections, pages, line numbers and figures refer to the version of our manuscript with changes highlighted (unless noted differently).

[multiple east Pacific sites; Dekens et al., 2007], and ~30 kyr [multiple EEP sites; Ford et al., 2012] *versus* ~750 yr [Site 849; this study] to ~3 kyr [Site 1241; Steph et al., 2006, 2010]) to resolve the "transient" thermocline state change during the ~2.7–2.5 Ma period as observed for Site 1241, if existent. Nevertheless, we hypothesize that records from Site 1241 reflect a more local signal than Site 849 and other sites located within the equatorial "cold tongue". Moreover, Site 1241 was possibly temporally affected by glacioeustatically induced openings and closures of the Central American Seaway around ~2.5 Ma (Marine Isotope Stages [MIS] 100–96): High-resolution (~1 kyr) data (surface-to-thermocline, i.e., *G. sacculifer*-to-*N. dutertrei,* Mg/Ca-based temperature gradient) from this site reveal changes in thermocline depth on glacial-interglacial timescales for MIS 100–96 (Groeneveld et al., 2014), while our records from Site 849 indicate no glacial-interglacial variability in thermocline depth for the same time interval (for details see our response to comment R.1.3, see also new Fig. 8 and Fig. S2.1 in our Response Letter to Reviewer #2).

To account for the reviewer's comment, a more detailed comparison of our new records on thermocline evolution at Site 849 to other thermocline data in the tropical east Pacific have been included in Section 5.4.1 (p. 10, line 23 to p. 11, line 3; p. 11, lines 10–21; see also new Fig. 8), focussing on both the "long-term" trend and also on the "transient" or glacial-interglacial variability. In this context, we also have modified Figure 1 by showing (in addition to the two maps already presented) a global map indicating the location of sites mentioned in the text. This will further enhance clarity for the readers.

R.1.3: "Additionally, the impact of the final stages of closing the Panamanian Gateway could still have been involved, both concerning productivity (Schneider and Schmittner, 2006) and thermocline structure; Groeneveld et al. (2014) also show thermocline *vs* surface temperatures for MIS 96–100 for east Pacific Site 1241. As Site 1241 is located outside the cold tongue, modern conditions show a strong sea water temperature gradient between both locations, but the long-term thermocline shoaling during the Pliocene occurred both in and outside the cold tongue area. A comparison would therefore also provide additional evidence for a change in intensity of upwelling/cold tongue or if the full east Pacific experienced these changes."

We thank the reviewer for this comment. The records of Groeneveld et al. (2014) suggest that water-column stratification (defined as the temperature difference between the surface-dwelling species *G. sacculifer* and the thermocline-dwelling species *N. dutertrei*) at east Pacific Site 1241 was higher during interglacials (temperature difference [ΔT] of ~3–4 °C) than during glacials (ΔT of ~1–2 °C) for MIS 100–96, thereby implying thermocline-state

changes on glacial-interglacial timescales (see new Fig. 8b; see also Fig. S2.1 in our Response Letter to Reviewer #2). This contradicts our new data from Site 849 where both surface-to-thermocline $\delta^{18}O$ and temperature gradients indicate no change in thermocline depth on glacial-interglacial timescales for MIS G6–96 (Figs. 7b and 8b). Together, data from Sites 849 and 1241 suggest that thermocline-state changes have not occurred homogenously across the entire tropical east Pacific, possibly due to the following reasons:

(i) Sites 849 and 1241 are located in different areas of the highly heterogeneous tropical east Pacific (i.e., cold tongue upwelling region [Site 849] *versus* warm pool [Site 1241]). Therefore it appears reasonable to hypothesize that changes in thermocline depth in- and outside the cold tongue upwelling regime simply underwent a different evolution on glacial-interglacial timescales. This hypothesis is supported by faunal data (calcareous nannofossil counts) from EEP cold tongue Site 846, which, like Site 849, do not indicate any variations in thermocline depth for MIS 101–95 (Bolton et al., 2010).

(ii) It is likely that Site 1241 reflects a more local signal due to influences by glacioeustatically induced openings and closures of the Central American Seaway during MIS 100–96 (as suggested by Groeneveld et al. [2014]), while Site 849 records a more open-ocean, quasi-global signal due to its position west of the East Pacific Rise (Mix et al., 1995). This is, for example, highlighted by the fact that global climate-ocean ecosystem model experiments (Schneider and Schmittner, 2006) indicate that a closure of the Central American Seaway helps to promote upwelling in nearby EEP regions (including Site 1241) – in contrast, Site 849 appears to be mostly unaffected by such changes as shown by sand-accumulation-rate-based primary productivity data (Jakob et al., 2016). However, it is likely, although speculative, that temporal closures of the Central American Seaway from MIS 100 through 96 (Groeneveld et al., 2014) might have contributed to generally increasing upwelling and thus primary productivity rates that have been observed at Site 849 since MIS 100 (Jakob et al., 2016; this study; Fig. 7c–d).

To account for this comment, we have included a discussion into Sections 5.4.1 (p. 10, line 23 to p. 11, line 3) and 5.4.2 (p. 12, line 35 to p. 13, line 3) on (i) thermocline data derived from Sites 849 and 1241 (also in comparison to other datasets from the east Pacific; for details see our response to comment R.1.2 by Reviewer #1 and to comments R.2.2 and R.2.3 by Reviewer #2; see also Fig. S2.1 in our Response Letter to Reviewer #2 and new Figs. 6 and 8), and on (ii) the impact of glacioeustatically induced openings and closures of the Central American Seaway to these sites.

R.1.4: "Contamination of the samples seems to be absent concerning Mg/Ca, but Mn/Ca values are relatively high. These values, however, are not uncommon in older sediments (Groeneveld et al., 2006; Schmidt et al. 2006); and for the Galapagos area Lea et al. (2005) linked higher Mn/Ca to volcanic particles. One way to check the character of the Mn is to perform reduction cleaning to see if Mn-oxyhydroxides are involved. Another possibility may be an actual bottom water signal. Mn/Ca is recently receiving increasing attention as a recorder of bottom water oxygen conditions, either in the sediment, as coatings involving $MnCO_3$ being formed onto the tests or in the foram calcite itself. If that is the case you may see glacial interglacial variability in the Mn/Ca and it may be linked to $\delta^{13}C$ as variations in productivity would change the intensity of the oxygen minimum zone."

We appreciate this comment. As highlighted in our manuscript, it is important to note that if Mn-rich overgrowths existed on *G. crassaformis* tests, they might change absolute temperature estimates by on average ~0.5 °C, but this would not affect the overall shape of the Mg/Ca-based temperature record (Fig. 4c, d). Therefore it appears reasonable to assume that early diagenetic Mn-rich overprinting has no significant impact on our interpretation regarding relative changes in the surface-to-thermocline gradient. Hence, we argue that for the purpose of our study the reductive cleaning step, which might remove such overgrowths, is not required. However, to account for the reviewer's comment, we have re-checked the character of Mn in/on *G. crassaformis* tests at our study site as follows:

(i) The reviewer suggests that Mn-oxyhydroxides might perhaps explain enhanced Mn/Ca ratios (~0.2–2.1 mmol/mol; Fig. 4) in *G. crassaformis* tests at our study site. We have tested this possibility through a modification of the cleaning procedure for element analyses via including an additional reductive cleaning step for selected samples (e.g., Barker et al., 2003). As a reductive reagent, a mixture of hydrazine, ammonium hydroxide and ammonium citrate was used. The results show by ~40–45 % lower Mn/Ca values for samples that were cleaned reductively compared to samples that underwent only oxidative cleaning (Fig. S1.1). This indicates that at least two different Mn phases coexist on *G. crassaformis* tests surfaces – perhaps Mn-oxyhydroxides that can be removed by reductive cleaning and another phase that can neither be removed by oxidative nor by reductive cleaning. To comply with the reviewer's comment, we have included this information into Section 5.2 (p. 7, lines 22–28).

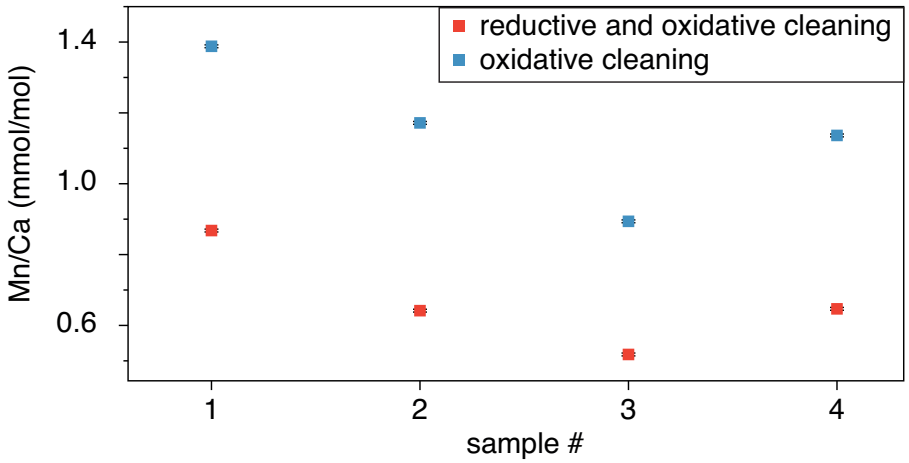

Figure S1.1: Evaluation of potential contaminations on *G. crassaformis* test surfaces from Site 849. Mn/Ca ratios of selected samples (1: 849D-7/3-77–79cm, 2: 849D-7/3-105–107cm, 3: 849D-7/4-51–53cm, 4: 849D-7/4-67–69cm) that underwent reductive and oxidative cleaning (red) or oxidative cleaning only (blue).

(ii) The reviewer is correct in stating that if foraminiferal Mn/Ca ratios trace bottom-water oxygen conditions (e.g., McKay et al., 2015; Koho et al., 2017), our Mn/Ca record should follow the glacial-interglacial cyclicity given by the productivity proxy record from the same site and time interval (Fig. 7d; Jakob et al., 2016). To identify coherencies between these two records (Mn/Ca values *versus* sand-accumulation rates; note that we use the latter record as a primary productivity proxy instead of commonly used foraminiferal $\delta^{13}C$ proxy data since $\delta^{13}C$ at Site 849 has been shown to not simply trace *in-situ* changes in productivity, but rather reflects the $\delta^{13}C$ signature imprinted on high-southern-latitude waters that are transported to the EEP [Jakob et al., 2016]) we performed Blackman-Tukey cross-spectral analyses with a 30 % overlap using the AnalySeries software package version 2.0.8 (Paillard et al., 1996). Data for cross-spectral analyses were linearly interpolated, detrended, and prewhitened.

Our results indicate that indeed both records yield a 41-kyr (i.e., glacial-interglacial) cyclicity (Fig. S1.2). However, the Mn/Ca and the productivity proxy records do not fluctuate in phase; instead, they are shifted by approximately -102° (equal to -11.5 kyr) for the 41 kyr period. If Mn/Ca reflects bottom-water oxygen concentrations, the oxygen (Mn/Ca) and productivity (sand-accumulation rate) proxy records are, however, expected to fluctuate in phase. Therefore we exclude that *G. crassaformis* Mn/Ca data at Site 849 record bottom-water oxygenation. We decided not to include this discussion into the manuscript as it goes far beyond the scope of our study, and we hope this finds approval of the editor.

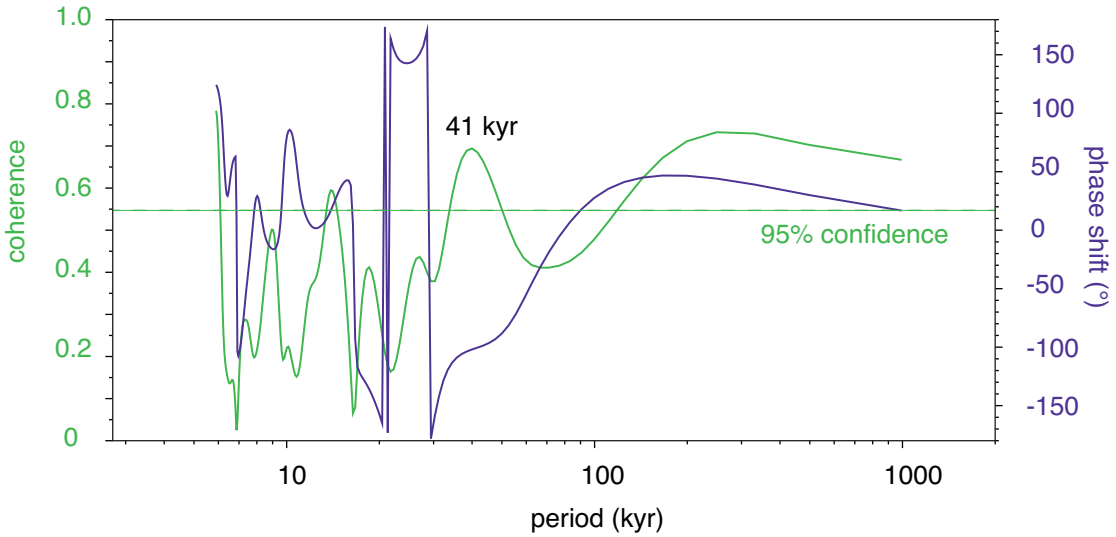

Figure S1.2. Blackman-Tukey cross-spectral analysis for the identification of phase shifts at Site 849 for the time interval from ~2.65 to 2.4 Ma. Coherence (green) and phase (purple) relationship between productivity (sand-accumulation rates [Jakob et al., 2016]) and Mn/Ca ratios are plotted on log scales. Negative values in this phase plot indicate that productivity lags Mn/Ca, i.e., by -102° (equal to -11.5 kyr) for the 41 kyr period.

(iii) Reviewer #1 suggests that enhanced Mn/Ca values in our samples could also be linked to volcanic particles (e.g., Lea et al., 2005). However, while carefully reading this study, we recognized that Lea et al. (2005) observed enhanced Fe/Ca and Al/Ca ratios (rather than increased Mn/Ca ratios) in planktic foraminifera from core intervals that were rich in volcanic debris. In contrast, they link higher Mn/Ca values to diagenetic coatings (Mn-carbonates) on foraminiferal tests. Moreover, we are unaware of any study that has shown a relation between foraminiferal Mn/Ca ratios and volcanic material. Therefore we decide to not include such a discussion into our manuscript.

R.1.5: "You distinguished between dextral and sinistral forms of *G. crassaformis* where possible. Based on a previous study there was no difference in the geochemical structure, but is the occurrence of both forms controlled by glacial-interglacial variability? Also, did you notice differences in the signature of more heavily encrusted specimens *vs* less encrusted specimens or even between different morphological types which occur during this period (Rögl 1974)?"

We preferentially selected the most abundant coiling direction (sinistral) of *G. crassaformis* tests at Site 849. However, the sinistral coiling forms did not occur continuously over the sampling interval. Thus, we also used the dextral coiling tests for some intervals, (~2.46–2.43 Ma [69.84–69.04 meters composite depth (mcd)], ~2.51–2.50 Ma [70.85–70.68 mcd]) and also for some specific time points (2.40 Ma [68.10 mcd], 2.41 Ma [68.32 mcd]). The oc-

currence of dextrally and sinistrally coiling *G. crassaformis* specimens, however, appears to be randomly rather than following a certain cyclicity.

Furthermore, we did not notice a change between heavily and less encrusted *G. crassaformis* specimens or even between different morphotypes throughout the investigated time interval while picking. Scanning Electron Microscope (SEM) images of *G. crassaformis* specimens derived from both glacial and interglacial samples also do not reveal such changes (Fig. 3).

To account for the reviewer's comment and to enhance clarity for the readers, we have modified the relevant sentences in Sections 4.1 (p. 4, lines 28–29) and 5.1 (p. 7, lines 6–9).

R.1.6: "Seasonality of *G. ruber*: Sediment trap studies often show a distinct seasonality in *G. ruber* fluxes when areas are affected by seasonal upwelling conditions. So this may mean that also in the cold tongue *G. ruber* is more inclined towards the season when upwelling decreases in intensity (Mohtadi et al., 2009; Jonkers and Kucera, 2015)."

In extratropical regions *G. ruber* most likely represents summer surface-water conditions (e.g., Schiebel and Hemleben, 2000; Schiebel et al., 2002), while in the tropics, where seasonal climate variability is low, plankton tow studies indicate that this species can be found year around and is therefore typically used as recorder for mean annual surface-water conditions (e.g., Deuser et al., 1981; Lin et al., 1997). This is supported by a study on global planktic foraminiferal shell fluxes that show that in waters with temperatures >25 °C (i.e., sea-surface temperatures [SSTs] prevailing at our study site during interglacials; Jakob et al. [2017]) *G. ruber* has a less predictable flux pattern with random peak timing (Jonkers and Kučera, 2015). In colder waters, seasonality appears to be more prominent, with decreasing fluxes when temperature decreases (Jonkers and Kučera, 2015). The reviewer is therefore correct in stating that *G. ruber* proxy data (particularly of glacial periods) might be biased towards the season with lower upwelling intensity. In contrast, however, Mohtadi et al. (2009) show that *G. ruber* fluxes in the upwelling region off south Java are not solely related to upwelling: Although this species consistently shows enhanced flux rates during the upwelling period, its flux rates are also temporarily as high during non-upwelling seasons.

In light of the above considerations, we find it reasonable to assume that *G. ruber* is a more likely recorder for mean surface-water conditions than for a particular season in the low-latitude EEP upwelling regime. To account for the reviewer's comment, relevant references have been added to Section 5.3 (p. 8, lines 7–14) and more detailed information on

seasonality at Site 849 is now provided (for details see our response to comment R.2.14 by Reviewer #2).

R.1.7: "Add bars in the figures to better be able to distinguish between glacial and interglacial time periods."

Bars as suggested by the reviewer had already been included in the figures of the original manuscript version. However, we have acted on this suggestion by highlighting the bars by a more prominent colour.

R.1.8: "Page 8, line 23: although in the case here with *G. ruber* and *G. crassaformis* living in different water masses, your $\delta^{18}O$ may also indicate a difference in salinity."

We fully agree with the reviewer and have revised this paragraph (Section 5.4.1, p. 10, lines 11–15).

References (other than those already cited in the discussion paper)

Deuser, W. G., Ross, E. H., Hemleben, C., and Spindler, M.: Seasonal changes in species composition, numbers, mass, size, and isotopic composition of planktonic foraminifera settling into the deep Sargasso Sea, Palaeogeogr., Palaeoclimat., Palaeoecol., 33, 103–127, 1981.

Koho, K. A., de Nooijer, L. J., Fontanier, C., Toyofuku, T., Oguri, K., Kitazato, H., and Reichart, G.-J.: Benthic foraminiferal Mn/Ca ratios reflect microhabitat preferences, Biogeosciences, 14, 3067–3083, 2017.

Lea, D. W., Pak, D. K., and Paradis, G.: Influence of volcanic shards on foraminiferal Mg/Ca in a core from the Galápagos region, Geochem., Geophys., Geosyst., Q11P04, doi:10.1029/2005GC000970, 2005.

McKay, C. L., Groeneveld, J., Filipsson, H. L., Gallego-Torres, D., Whitehouse, M. J., Toyofuku, T., and Romero, O. E.: A comparison of benthic foraminiferal Mn/Ca and sedimentary Mn/Al as proxies of relative bottom-water oxygenation in the low-latitude NE Atlantic upwelling system, Biogeosciences, 12, 5415–5428, 2015.

Rögl, F.: The evolution of the *Globorotalia truncatulinoides* and *Globorotalia crassaformis* group in the Pliocene and Pleistocene of the Timor Through, DSDP Leg 27, Site 262, Init. Repts., 27, Washington, 1974.

Schiebel, R., and Hemleben, C.: Modern planktic foraminifera. Paläontologische Zeitschrift, 79, 135–148, 2005.

Schiebel, R., Schmuker, B., Alves, M., and Hemleben, C.: Tracking the recent and late Pleistocene Azores front by the distribution of planktic foraminifers. J. Marine Syst., 37, 213–227, 2002.

Response to Reviewer #2

R.2.1: "The paper by Jakob et al focusses on a new high resolution paleoceanographic record of the onset of the large Northern Hemisphere Glaciations at the Plio-Pleistocene transition 2.6 Myrs ago. The authors have documented changes in the surface hydrography at Site 849, in the Eastern Equatorial Pacific, based on coupled $\delta^{18}O$ and Mg/Ca in *G. ruber*, record mostly published in previous papers by the same group, and compare this record with a new *G. crassaformis* $\delta^{18}O$/Mg/Ca record interpreted as a deep-thermocline species. Those geochemical datasets are augmented with a record of sediment fluxes and with some countings of *G. crassaformis* and *G. menardii/G. tumida*. Using the difference in the temperature records and $\delta^{18}O$, the authors describe what they think changes in the EEP thermocline, with a thermocline shoaling until 2.55 Myr followed by a stable thermocline. The article is a welcome addition as it does document in the EEP a Mg/Ca record for a deep-dwelling species.

The manuscript is well written and the figures are also generally well crafted. As this is the third manuscript on the same record, the paper also details what are the novelties compared to the previous records. I do feel that the technical issues are well thought out, e.g. the potential impact of Mn crusts on the Mg composition of the foraminiferal calcite is ruled out with some backed up arguments (but missing the Pena et al., 2005 study which worked in the EEP to estimate the impact of these crusts on the Mg/Ca of foraminifera). On the choice of the calibration used, the authors are also quite careful, and do pick the Cléroux et al. calibration quite sensibly."

We thank the reviewer for this positive assessment. The study by Pena et al. (2005) is now included (Section 5.2, p. 7, lines 25–28)*.

R.2.2: "My main comment on the manuscript, is that it does miss a real discussion. Symptomatically, the authors did not compare their records to any other records either from the same region or from more remote sites, which would have lent some weight to their hypothesis."

We agree with Reviewer #2 and acknowledge that our original manuscript has not presented a comparison of thermocline data from our study site with other datasets revealing thermocline evolution for the same time interval. To account for this comment made by both reviewers, we now have compared thermocline data from Site 849 to the following datasets of the same time interval (Section 5.3.2, p. 9, lines 8–27; Section 5.4.1, p. 10, line 25 to p. 11, line 3; Section 5.4.1, p. 11, lines 10–21; to provide maximum clarity for the readers, we also have

* Sections, pages, line numbers and figures refer to the version of our manuscript with changes highlighted (unless noted differently).

modified Figure 1 by showing – in addition to the two maps already presented – a global map indicating the location of all sites that are mentioned in the text):

(i) Geochemical ($\delta^{18}O$ and Mg/Ca) data of *G. crassaformis* from eastern tropical Indian Ocean Site 214 (Karas et al., 2009; Fig. S2.1c and new Fig. 6b). For a detailed discussion see our response to comment R.2.3.

(ii) Geochemical ($\delta^{18}O$ and Mg/Ca) data of *G. tumida* from eastern tropical Pacific Site 1241 (Steph et al., 2006a, 2010; Fig. S2.1c and new Figs. 6b and 8a). For a detailed discussion see our response to comment R.1.2 by Reviewer #1.

(iii) Surface-to-thermocline (*G. sacculifer* to *N. dutertrei*) Mg/Ca-based temperature gradients from eastern tropical Pacific Site 1241 (Groeneveld et al., 2014; Fig. S2.1a,b and new Figs. 6c and 8b). For a detailed discussion see our response to comment R.1.3 by Reviewer #1.

(iv) Alkenone-based sea-surface temperatures (SSTs) from Site 1090 in the Southern Ocean (i.e., the source region for waters upwelled in the Eastern Equatorial Pacific [EEP]) (Martínez-Garcia et al., 2010). For a detailed discussion see our response to comment R.2.3.

We note that in comparison to the Mg/Ca-based temperature data of *G. tumida* yet available for our study site and target interval (~15.5–17.5 °C; Ford et al. [2012]; Fig. S2.1c and new Fig. 6b) our *G. crassaformis* temperatures (1.0–11.6 °C) appear to be relatively low. The *G. tumida*-based temperature record of Ford et al. (2012) is, however, of low temporal resolution, with only six datapoints for the 2.75–2.4 Ma interval. Therefore we argue that this comparison is not robust enough to warrant further discussion in the revised version of the manuscript.

R.2.3: "The Mg/Ca values measured in *G. crassaformis* are quite low, and give some very low temperature range, mostly between 1 to 6 °C (regardless of the calibration used is the one by Cléroux or the one by Regenberg). Those temperatures appear to be even colder than modern temperature at the sites, and it is unlikely that the LGM temperatures were much colder than 1. I am thus puzzled by those extremely low temperatures, though one might argue that they are close to the Tcrassa inferred at site DSDP214. Moreover the temperatures at the site 849 are much colder than surface subantarctic waters during the same time interval (site 1090). I would like to have some sense of the process by which the water masses where *G. crassaformis* do live would be much colder in the equatorial Pacific than in subantarctic waters."

We agree with Reviewer #2 that temperatures reconstructed from *G. crassaformis* (~1–11.6 °C; Fig. 5d) are difficult to reconcile with

(i) thermocline temperatures of the Last Glacial Maximum in the eastern tropical Pacific (~14 to 16 °C inferred from Mg/Ca data of *N. dutertrei* from the Cocos and Carnegie Ridges [Hertzberg et al., 2016] and of *G. tumida* from Site 849 [Ford et al., 2015], respectively);

(ii) modern bottom-water temperatures at our study site of about ~1.5 °C (Locarnini et al., 2013) – note that because the exact calcification depth of *G. crassaformis* in the EEP remains unclear, a direct comparison to modern temperatures of an assumed *G. crassaformis* calcification depth (~400–800 m, equal to ~5–8 °C at Site 849; Fig. 1c) is not straight forward (for details see our response to comment R.2.15);

(iii) SSTs of ~10.5–17 °C during our study interval at Site 1090 (Martínez-Garcia et al., 2010) in the Southern Ocean that provides source waters for the EEP upwelling region (we are aware that Site 1090 is not on the direct trajectory from the Southern Ocean to the EEP; however, this site is accepted as the best end member of Southern Ocean waters currently available [Billups et al., 2002; Pusz et al., 2011]).

Although our temperature record of *G. crassaformis* appears to be too cold in comparison to the above-mentioned data, it is close to the temperature range inferred for Site 214 in the tropical eastern Indian Ocean for the same species and time interval (~8–10 °C; Karas et al, 2009; Fig. S2.1 and new Fig. 6b). This makes it reasonable to assume that our *G. crassaformis*-based temperature record indeed reflects realistic values. However, thermocline temperatures of ~1–11.6 °C at low-latitude Sites 214 and 849 are difficult to reconcile with SSTs of ~10.5–17 °C at high-southern-latitude Site 1090 during the same time interval. This temperature difference implies that there must have been substantial cooling of Southern Ocean surface-waters (i) either when being downwelled and transported to the lower latitudes and/or (ii) through mixing with Antarctic Bottom Waters, which presently has a bottom-water temperature of about 0 °C (Craig and Gordon, 1965). In this context, it is important to note that very low *G. crassaformis*-based temperatures at Site 849 of ~1 °C result from only one datapoint, while temperatures typically higher than 2–3 °C during the remaining target interval even during most prominent glacials of the intensification of Northern Hemisphere Glaciation can be reconciled better with the mixing hypothesis presented above.

To account for the reviewer's comment, we have elaborated on absolute temperature estimates derived from *G. crassaformis* in comparison to other datasets (Section 5.3.2, p. 9, line 8 to p. 10, line 4).

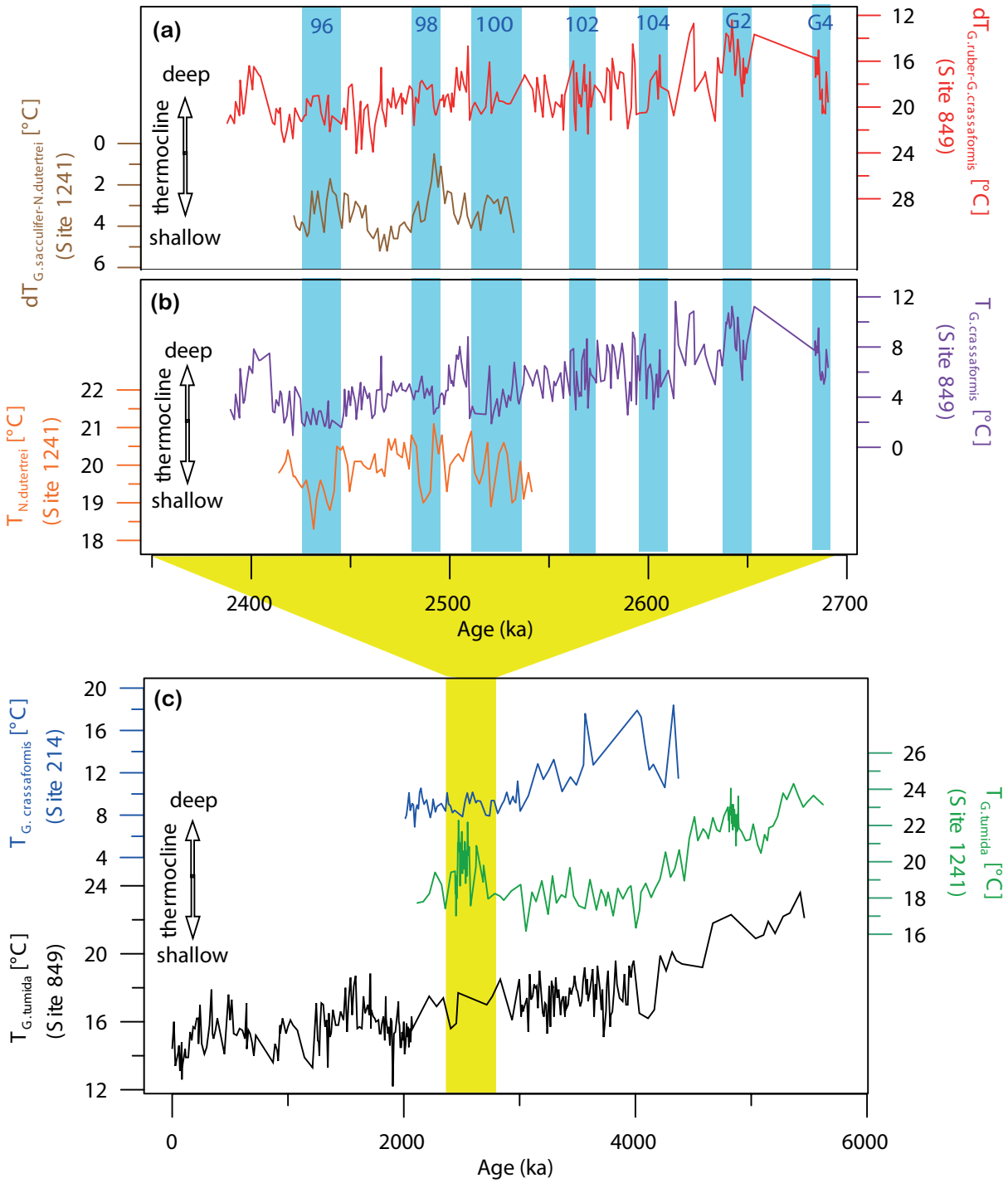

Figure S2.1: Comparison of thermocline proxy records. (a) Stratification data (surface-to-thermocline temperature gradient) for Site 849 in the EEP upwelling regime (this study; red) and Site 1241 in the East Pacific Warm Pool (Groeneveld et al., 2014; brown) for ~2.7–2.4 Ma. (b) Thermocline temperatures based on *G. crassaformis* at Site 849 in the EEP upwelling regime (this study; purple) and based on *N. dutertrei* at Site 1241 in the East Pacific Warm Pool (Groeneveld et al., 2014; orange) for ~2.7–2.4 Ma (c) Thermocline temperatures from Site 214 in the tropical eastern Indian Ocean (based on *G. crassaformis*; Karas et al., 2009; blue), Site 1241 in the East Pacific Warm Pool (based on *G. tumida*; Steph et al., 2006a; green) and Site 849 in the EEP upwelling regime (based on *G. tumida*; Ford et al., 2012; black) for the past ~6 Myr. Blue bars in (a) and (b) highlight glacial periods. Yellow bar in (c) marks our study interval.

R.2.4: "The location of the Site ODP849 is at the edge of the cold tongue. Deglacial studies have shown that this cold tongue did migrate both longitudinally, but also latitudinally (e.g. Koutavas et al. 2003). I wonder if one might not interpret the subtle changes in the record as a long term shift the EEP rather than a subsurface process."

We agree that there is a migration of the cold tongue over glacial-interglacial timescales that can be reconstructed using an approach as exemplified in the study of Koutavas et al. (2003). For the studied time interval, however, the amount of sites (both with the required temporal resolution and preservation of foraminiferal tests) that would be required for such a study is simply not available. Furthermore, the migration mentioned by Reviewer #2 occurs on a glacial-interglacial timescale, while the changes inferred from our data show no significant changes on these short timescales, but rather a long-term shift in thermocline depth. Therefore, we acknowledge the comment of Reviewer #2, but are unfortunately not able to include this kind of information in our contribution.

R.2.5: "I am puzzled by the number of *G. crassaformis* found in the record, reaching at sometimes close to 30 % of the >250 µm. Though the comparison with modern and LGM census of planktonic foraminifera is not straight forward, as late Pleistocene counts are based on the >150 µm fraction, I am surprised that core-top data show extremely low percentages of *G. crassaformis* (typically below 1 %, exceptionally reaching 5 %), far less with results from this study. I understand that the authors do have some arguments that the dissolution is limited at this site (fragmentation index for example), yet I cannot find an alternate process that would selectively get rid of most of the surface to subsurface species."

We respectfully disagree with the reviewer that high percentages of *G. crassaformis* within the planktic foraminiferal assemblage observed at Site 849 can only be explained by selective dissolution of less resistant planktic foraminifera such as *Globigerinoides* (Dittert et al., 1999). The overall good preservation and lack of significant changes in preservation between glacials and interglacials (Fig. 3) along with the low fragmentation index (Jakob et al., 2017) argue against preservation playing a significant role. Another possibility might be that living conditions (e.g., oxygen content in case of *G. crassaformis* [Jones, 1967; Kemle von Mücke and Hemleben, 1999]) changed over time. In our manuscript we argue that increasing *G. crassaformis* abundances from ~2.64 Ma (MIS G2) onward (Fig. 7c) can be explained by changing environmental conditions that were more favourable for this species. This line of argument can also be used to explain lower percentages of *G. crassaformis* in the modern as

opposed to our target interval assuming less favourable living conditions. To account for the reviewers comment, we have included this information in Section 5.4.2 (p. 12, lines 1–4)

R.2.6: "The ΔT record does not show any glacial/interglacial dynamics. This is quite surprising as there are a large number of studies (modelling and observational) that have shown some changes in the thermocline depth during the most recent glacial/interglacial transitions. I wonder then if the choice of picking a quite deep species (see below) and a shallow species such as *G. ruber* does really reflect changes in the thermocline. Species such as *G. tumida, G. menardii,* or *N. dutertrei* living closer to the thermocline would have been more sensitive to changes. I would therefore be grateful if the authors could add some lines on how they can groundcheck their proxy of the thermocline?"

Again, we thank the reviewer for this constructive comment. First, we want to shed light onto the applicability of our approach for surface-to-thermocline (i.e., *G. ruber* to *G. crassaformis*) gradient calculation. Subsequently, we present a more detailed discussion of our ΔT record also in comparison to previous studies:

(i) To reconstruct thermocline changes, we decided to focus on $\delta^{18}O$ and temperature gradients between sea-surface and thermocline waters. *Globigerinoides ruber* lives in the mixed layer, and as one of the shallowest-dwelling species among modern planktic foraminifera it is typically used as recorder for surface-water (mixed-layer) conditions (e.g., Dekens et al., 2002; Rippert et al., 2016); therefore we decided for this species as surface-water recorder.

As a recorder for thermocline waters, we selected *G. crassaformis* because ongoing studies suggest that this species is rather conservative in its preferred calcification depths, although the life cycle of deep-dwelling planktic foraminifera can involve a vertical migration through the water column of several hundred meters. Instead, *G. crassaformis* specimens are suggested to mainly calcify below the thermocline (Regenberg et al., 2009, Steph et al., 2009, and references therein) by maintaining a more constant depth habitat near the base of the thermocline through time compared to other deep-dwellers (Cléroux and Lynch-Stieglitz, 2010). Therefore, it is reasonable to assume that this species is a suitable recorder for deep-thermocline conditions, which led us to compare surface-water records of *G. ruber* to records of the deep-thermocline-dwelling species *G. crassaformis* rather than to intermediate-dwelling species such as *G. tumida*, *G. menardii*, or *N. dutertrei* as a proxy for thermocline state changes.

Moreover, the selected approach has been successfully applied to previous studies on surface-water structure and thermocline evolution (e.g., Karas et al., 2009; Bahr et al., 2011). To account for the reviewer's comment and to enhance clarity for the readers, we have included information on the overall applicability of the selected approach for tracing thermocline changes into Section 5.4.1 (p. 10, lines 15–20).

(ii) The reviewer is correct in stating that a number of previous studies showed thermocline changes on glacial-interglacial timescales across the Last Glacial Maximum in the tropical Pacific. However, it remains unclear whether the thermocline shoaled (e.g., Andreasen and Ravelo, 1997; Lynch-Stieglitz et al., 2015) or deepened (DiNezio et al., 2011) during the Last Glacial Maximum. Across our study interval, there are both model- and proxy-based studies that indicate no glacial-interglacial changes in thermocline depth in the EEP (Lee and Poulson, 2005; Bolton et al., 2010; Jakob et al., 2017). In accordance with these studies, we therefore suggest that our new ΔT (and $\Delta\delta^{18}O$) records indeed reflect a true signal of thermocline development for the EEP cold tongue, i.e., no change in thermocline depth on the glacial-interglacial timescale during the late Pliocene to early Pleistocene (Fig. 7b). Instead, work of Groeneveld et al. (2014), which hints at glacial-interglacial changes in thermocline depth at Site 1241 (Fig. S2.1 and new Fig. 8b), is based on a site located outside the equatorial upwelling regime. Data from this site might reflect a more local signal than sites from the EEP cold tongue, possibly rather being related to glacioeustatically induced openings and closures of the Central American Seaway during that time (for details see our response to comment R.1.3 by Reviewer #1).

To account for the comment of Reviewer #2, we have extended the paragraph dealing with the glacial-interglacial evolution of the thermocline at Site 849 and its comparison to other datasets from the same time interval (Section 5.4.1, p. 10, line 21 to p. 11, line 3).

R.2.7: "The living depth of *G. crassaformis* in this study is supposed to be within the 500 to 1000 m range. To set the record straight, the authors have to be clear that they think that the "calcification range" of *G. crassaformis* is within this range. All the studies quoted by the paper to posit this range come from surface sediment samples, in which the authors have made the assumption that the isotopic temperature reflects the calcification depth. This is different from the actual mean living depth. As a couple of examples, the paper by Jones (1967) in the equatorial Atlantic did find most *G. crassaformis* at depths ranging 200 to 300 meters, not below 500 meters. The authors also quote Wejnert et al. 2013 indicating a calcification

depth below 500 meters. This is not what the paper states, as they indicate that the range is above 300 meters. Please correct accordingly."

We agree with Reviewer #2 and have to acknowledge that we incorrectly mixed the terms "habitat depth" and "calcification depth"; the relevant paragraph have been corrected when revising our manuscript as follows (Section 3, p. 3, lines 23–32):

(i) In accordance with our response to comment R.2.6, we state that *G. crassaformis* lives at the bottom of the thermocline (Niebler et al., 1999; Regenberg et al., 2009, Steph et al., 2009, and references therein) with a rather conservative calcification depth as opposed to other deep-dwelling foraminiferal species (Cléroux and Lynch-Stieglitz 2010).

(ii) Since the exact calcification depth of *G. crassaformis* in the EEP is unclear, we use calcification depths of this species determined by $\delta^{18}O$ values in the (sub-)tropical Atlantic and Caribbean Sea (~400 to 800 m water depth) (Steph et al., 2006b; Regenberg et al., 2009; Steph et al., 2009; Cléroux et al., 2013).

R.2.8: "note [page 2]: One might also consider the last major tipping climate history: The Holocene to Anthropocene transition or the last deglaciation. Please reword more carefully."

We agree with Reviewer #2 and have reworded the relevant sentences as suggested (Abstract, p. 1, lines 9–10; Section 1, p. 2, lines 5–6).

R.2.9: "note [page 2]: I would tend to think that it is not the shallow depth of the thermocline that exerts a role in the ENSO, but rather the reverse. So please reword in thinking the Eastern Pacific Ocean as a part of the ocean where atmospheres and surface oceanic layers are subtlety interconnected."

Again, we agree with the reviewer and have rephrased the respective paragraphs in the abstract and introduction as suggested (Abstract, p. 1, lines 12–14; Section 1, p. 2, lines 11–14).

R.2.10: "note [page 2]: I understand the framing in two alternate hypotheses, but there is also a mid-ground solution where the state of the equatorial Pacific did play a substantial role, without being the main climatic ruler. Moreover, if one would really test the role of the EEP, he would have to reconstruct the dynamics of the equator to pole gradient."

Indeed, such a test of the role of the EEP would require a much larger dataset and comparison to other sites and records. Since this would be beyond the scope of our contribution, we have carefully rephrased the respective sentences within our manuscript to account for this comment by Reviewer #2.

R.2.11: "note [page 2]: 'We use planktic (both sea-surface- and thermocline-dwelling) foraminiferal geochemical (^{18}O, ^{13}C and Mg/Ca) proxy records in combination with sedimentlogical (sand-accumulation rates) and faunal (abundance data of thermocline-dwelling foraminiferal species) information to reconstruct thermocline depth for the final phase of the late Pliocene/early Pleistocene iNHG from 2.75 to 2.4 Ma (MIS G7–95)': This final sentence of the introduction, which sums up the methods should be either moved in the methods, or argumented."

In line with the reviewer's comment, this paragraph has been moved to Section 4 (p. 4, lines 2–6)

R.2.12: "note [page 6]: The use of this very large size fraction is not regularly used. Could you elaborate on this choice?"

We are admittedly not sure if Reviewer #2 refers to the size fraction of *G. crassaformis* tests (315–400 µm) used for geochemical analyses or the size fraction selected for foraminiferal abundance counts (>250 µm). Therefore we will briefly elaborate on both aspects in the following:

(i) Geochemical analyses of *G. crassaformis* tests (315–400 µm):

A study that explores the relationship between the shell size of *G. crassaformis* and $\delta^{18}O$, $\delta^{13}C$ and Mg/Ca shows less variations for all parameters for the >300 µm fraction as opposed to the <300 µm fraction (Elderfield et al., 2002) and validates the use of a size fraction >300 µm. Finally, the 315–400 µm fraction has been selected in order to keep ontogenetic effects as small as possible (Elderfield et al., 2002; Friedrich et al., 2012), but at the same time to allow a sufficient number of *G. crassaformis* tests per sample. Moreover, the selected size fraction has also typically been used for geochemical analyses of *G. crassaformis* tests in earlier studies (e.g., Steph et al., 2006b; Karas et al., 2009).

It is further important to note that the geochemical records of *G. crassaformis* presented in Jakob et al. (2016) to be complemented in this study are based on the 315–400 µm size fraction as well. To remain consistent, we used the same size fraction in this study. To provide maximum clarity for the readers, we the relevant sentences have been rephrased (Section 4.1, p. 4, lines 20–23).

(ii) Foraminiferal abundance counts (>250 µm):

There are studies in which the >250 µm fraction is used for abundance counts of thermocline-dwelling species (e.g., Sexton and Norris, 2008). However, the reviewer is correct in stating that for abundance counts of the entire planktic foraminiferal assemblage (i.e.,

thermocline- and surface-dwelling species) smaller fractions (>63 µm or >125 µm) are typically investigated (e.g., Jehle et al., 2015; Luciani et al., 2017). The use of different size fractions for the purpose of abundance counts on thermocline-dwelling *versus* all planktic species is justified by the fact that test sizes are typically larger (smaller) in thermocline-dwelling (surface-dwelling) species (e.g., Davis, et al., 2013, and references therein; Feldmeijer et al., 2015). To account for the reviewer's comment, relevant references have been added (Section 4.2.5, p. 6, line 23).

R.2.13: "note [page 7]: A low fragmentation index might also correspond to the selective preservation of only resistant species. Please rephrase this sentence."
The reviewer is correct in stating that a low planktic foraminiferal fragmentation index might indicate either a good preservation of the entire planktic foraminiferal assemblage or the selective preservation of only resistant species, while less resistant species have been dissolved. However, we suggest that a low planktic foraminiferal fragmentation index at Site 849 indicates a generally good foraminiferal preservation, because also less resistant species such as *Globigerinoides* (see for example Tab. 1 in Dittert et al., 1999) occur in large numbers in these samples and are also well preserved (Fig. 3). Instead, if a low planktic foraminiferal fragmentation index indicated selective preservation of only resistant species, a substantially reduced number of *Globigerinoides* (and a poor preservation state of those individuals preserved) would be expected.

To account for the reviewer's comment, the relevant sentence in Section 5.1 (p. 7, lines 10–13) has been rephrased as suggested.

R.2.14: "note [page 7]: Please be more specific: What is the seasonality at the location of the site? Even though it might be significantly different, it cannot be ruled out without testing it."
Modern seasonal changes in SSTs at Site 849 have an amplitude of about ~0.4 °C (~24 °C during summer [June] *versus* ~23.6 °C during winter [January]; Locarnini et al. [2013]). The same seasonality (amplitude of ~0.4 °C) has been observed for 20 m water depth (Locarnini et al., 2013), i.e, the assumed mean depth habitat of the herein investigated foraminiferal species *G. ruber* (Wang, 2000). Determining seasonal temperature variations at a depth corresponding to the calcification depth of *G. crassaformis* is not straight forward since its calcification depth remains uncertain in the EEP (for details see our response to comment R.2.15). We suggest, however, seasonality to decrease with increasing water depth and therefore to be less than ~0.4 °C.

The above-mentioned data indicate that seasonal temperature variability is relatively low at our study site; therefore the geochemical signatures of the investigated foraminiferal species are considered not to be seasonally biased (Lin et al., 1997; Tedesco et al., 2007; Mohtadi et al., 2009; Jonkers and Kučera, 2015). As suggested by the reviewer, more specific information on seasonality at our study site as described above have been added to Section 5.3 (p. 8, lines 7–14).

R.2.15: "note [page 8]: What is the mean temperature at the site?"

Modern mean annual SSTs at Site 849 are ~23.5 °C (Locarnini et al., 2013) at 20 m water depth, i.e., the assumed mean depth habitat of *G. ruber* (Wang, 2000) (see also Fig. 1c). Mean SSTs reflected by *G. ruber* (~24 °C [Jakob et al., 2017]) indicate slightly warmer values, supporting the overall notion of a warmer-than-present EEP during the late Pliocene and early Pleistocene (e.g., Lawrence et al., 2006; Groeneveld et al., 2014). A comparison between modern and reconstructed Plio-/Pleistocene SSTs at Site 849 has already been presented in Jakob et al. (2017) and therefore will not be repeated in our manuscript.

While the depth habitat of *G. ruber* is relatively well understood (e.g., Wang, 2000) and therefore a comparison of *G. ruber*-based temperature estimates with modern values is possible, a comparison of *G. crassaformis*-based temperatures with modern values is not straight forward since the calcification depth of this species in the EEP has yet remained unclear. In the (sub-)tropical Atlantic, *G. crassaformis* typically calcifies between 400 and 800 m water depth (Steph et al., 2006b; Regenberg et al., 2009; Steph et al., 2009, and references therein; Cléroux et al., 2013). Assuming the same calcification depth range for this species in the EEP, this corresponds to a modern temperature range of about ~5–8 °C (Fig. 1c). *Globorotalia crassaformis*-based temperatures reconstructed for our study interval are similar to or somewhat higher than these values until MIS 100 (~5–15 °C); thereafter, thermocline temperatures became somewhat lower (~0–10 °C) (Fig. 5d). This would indicate that thermocline temperatures of the late Pliocene (early Pleistocene) were slightly higher (lower) than modern values, reflecting an overall warmer-than-present (colder-than-present) EEP at thermocline depth. We are fully aware that this comparison is not straight forward in light of the uncertainties in the calcification depth of *G. crassaformis*. Therefore we decided not to include this comparison (i.e., modern *versus* late Pliocene/early Pleistocene thermocline temperatures) into our manuscript.

R.2.16: "note [table1 page 17]: Add the number of samples processed for each site and study to give a sense of the effort included in this study."

We appreciate this suggestion. We now have included the number of samples processed (dried, weighed, washed) and geochemically analysed ($\delta^{13}C$, $\delta^{18}O$, Mg/Ca) per study (Tab. 1). Note that the number of samples analysed is somewhat lower than the number of samples processed depending on the availability of foraminiferal (*G. crassaformis* and *G. ruber*) material.

R.2.17: "note [Figure 1 page 18, panel B]: A latitudinal transect would be more useful to test whether the front did change as in Koutavas et al."

We agree with Reviewer #2 that a latitudinal transect would be more useful to test changes in the frontal position. Given the amount of data that would be needed for such an approach, however, this would be clearly beyond the scope of this contribution (see also our response to comment R.2.4).

References (other than those already cited in the discussion paper)

Andreasen, D. J., and Ravelo, A. C.: Tropical Pacific Ocean thermocline depth reconstructions for the last glacial maximum, Paleocenaography, 3, 395–413, 1997.

Bahr, A., Nürnberg, D., Schönfeld, J., and Garbe-Schönberg, D.: Hydrological variability in Florida Straits during Marine Isotope Stage 5 cold events, Paleoceanography, 26, PA2214, doi:10.1029/2010PA002015, 2011.

Billups, K., Channell, J. E. T., and Zachos, J.: Late Oligocene to early Miocene geochronology and paleoceanography from the subantarctic South Atlantic. Paleoceanography, 17(1), 1004, doi:10.1029/2000PA000568, 2002.

Cléroux, C., and Lynch-Stieglitz, J.: What caused G. truncatulinoides to calcify in shallower water during the early Holocene in the western Atlantic/Gulf of Mexico?, IOP Conf. Ser. Earth Environ. Sci., 9, doi:10.1088/1755-1315/9/1/012020, 2010.

Craig, H., and Gordon, L. I.: Deuterium and oxygen-18 variations in the ocean and the marine atmosphere, in: Stable isotopes in oceanographic studies and paleotemperatures, edited by: Tongiorgi, E., Spoletto, Pisa, 9–130, 1965.

Davis, C. V., Badger, M. P. S., Bown, P. R., and Schmidt, D. N.: The response of calcifying plankton to climate change in the Pliocene, Biogeosciences, 10, 6131–6139, 2013.

DiNezio, P. N., Clement, A., Vecchi, G. A., Soden, B., Broccoli, A. J., Otto-Bliesner, B. L., and Braconnot, P.: The response of the Walker circulation to Last Glacial Maximum forcing: Implications for detection in proxies, Paleoceanography, 26, PA3217, doi:10.1029/ 2010PA002083, 2011.

Dittert, N., Baumann, K.-H., Bickert, T., Henrich, R., Huber, R., Kinkel, H., and Meggers, H.: Carbonate dissolution in the deep-sea: Methods, quantification and paleoceanographic application, in: Use of Proxies in Paleoceanography, edited by: Fischer, G. and Wefer, G., Springer, New York, 255–284, 1999.

Feldmeijer, W., Metcalfe, B., Brummer, G.-J. A., and Ganssen, G. M.: Reconstructing the depth of the permanent thermocline through the morphology and geochemistry of the deep dwelling planktonic foraminifer *Globorotalia truncatulinoides*, Paleoceanography and Paleoclimatology, 30, doi:10.1002/2014PA002687, 2015.

Ford, H. L., Ravelo, A. C., Polissar, P. J.: Reduced El Niño–Southern Oscillation during the Last Glacial Maximum, Science, 347, 255–258, 2015.

Hertzberg, J. E., Schmidt, M. W., Bianchi, T. S., Smith, R. W., Shields, M. R., and Marcantonio, F.: Comparison of eastern tropical Pacific TEX_{86} and *Globigerinoides ruber* Mg/Ca derived sea surface temperatures: Insights from the Holocene and Last Glacial Maximum, Earth Planet. Sci. Lett, 434, 320–332, 2016.

Jehle, S., Bornemann, A., Deprez, A., and Speijer, R. P.: The impact of the Latest Danian Event on planktic foraminiferal faunas at ODP Site 1210 (Shatsky Rise, Pacific Ocean), PLoS One, doi:10.1371/journal.pone.0141644, 2015.

Karas, C., Nürnberg, D., Gupta, A. K., Tiedemann, R., Mohan, K., and Bickert, T.: Mid-Pliocene climate change amplified by a switch in Indonesian subsurface throughflow. Nat. Geosci., 2, 434–438, 2009.

Karas, C., Nürnberg, D., Tiedemann, R., and Garbe-Schönberg, D.: Pliocene climate change of the Southwest Pacific and the impact of ocean gateways, Earth Planet. Sci. Lett, 301, 117–124, 2011.

Luciani, V., D'Onofrio, R. D., Dickens, G. R., and Wade, B. S., Planktic foraminiferal response to early Eocene carbon cycle perturbations in the southeast Atlantic Ocean (ODP Site 1263), Global Planet. Change, 158, 119– 33, 2017.

Lynch-Stieglitz, J., Polissar, P. J., Jacobel, A. W., Hovan, S. A., Pockalny, R. A., Lyle, M., Murray, R. W., Ravelo, A. C., Bova, S. C., Dunlea, A. G., Ford, H. L., Hertzberg, J. E., Wertman, C. A., Maloney, A. E., Shackford, J. K., Wejnert, K., and Xie, R. C.: Glacial-interglacial changes in central tropical Pacific surface seawater property gradients, Paleoceanography, 30, doi:10.1002/2014PA002746, 2015.

Martínez-Garcia, A., Rosell-Melé, A-. McClymont, E. L., Gersonde, R., and Haug, G. H.: Subpolar link to the emergence of the modern equatorial Pacific cold tongue, Science, 328, 5985, 1550–1553, 2010.

Pusz, A. E., Thunell, R. C., and Miller, K. G. (2011). Deep water temperature, carbonate ion, and ice volume changes across the Eocene-Oligocene climate transition. Paleoceanography, 26, PA2205, doi:10.1029/2010PA001950, 2011.

Sexton, P. F., and Norris, R. D.: Dispersal and biogeography of marine plankton: Long-distance dispersal of the foraminifer *Truncorotalia truncatulinoides*, Geology, 36, 899–902, 2008.

List of relevant changes

Reviewer comment	Subject	Changes made to account for the reviewer's comments*
R.1.1, R.1.2, R.2.2, R.2.3	Interaction with other studies	Section 5.3.2, p. 9, line 8 to p. 10, line 4; Section 5.4.1, p. 10, line 23 to p. 11, line 3; Section 5.4.1, p. 11, lines 10–21; Section 5.4.2, p. 12, lines 6–10; Section 5.4.2, p. 13, lines 3–14; new Figs. 1, 6, 8
R.1.3	Impact of Panamanian Gateway	Section 5.4.1, p. 10, line 23 to p. 11, line 3; Section 5.4.2, p. 12, line 35 to p. 13, line 3
R.1.4, R.2.1	*G. crassaformis* test contamination	Section 5.2, p. 7, lines 22–28
R.1.5	*G. crassaformis* morphometry	Section 4.1, p. 4, lines 28–29; Section 5.1, p. 7, lines 6–9
R.1.6, R.2.14	Seasonality	Section 5.3, p. 8, lines 7–14
R.2.5	High *G. crassaformis* percentages compared to modern core-top samples	Section 5.4.2, p. 12, lines 1–4
R.2.6	Groundcheck of thermocline proxy	Section 5.4.1, p. 10, lines 15–20
R.2.7	"living depth" *versus* "calcification depth"	Section 3, p. 3, lines 23–32
R.2.12	*G. crassaformis* size fraction for geochemical analyses	Section 4.1, p. 4, lines 20–23
R.2.12	Size fraction for foraminiferal abundance counts	Section 4.2.5, p. 6, line 23

*Sections, pages, line numbers and figures refer to the version of our manuscript with changes highlighted.

Thermocline state change in the Eastern Equatorial Pacific during the late Pliocene/early Pleistocene intensification of Northern Hemisphere Glaciation

Kim A. Jakob[1], Jörg Pross[1], Christian Scholz[1], Jens Fiebig[2], Oliver Friedrich[1]

[1]Institute of Earth Sciences, Heidelberg University, 69120 Heidelberg, Germany
[2]Institute of Geosciences, Goethe-University Frankfurt, 60438 Frankfurt, Germany

Correspondence to: Kim A. Jakob (kim.jakob@geow.uni-heidelberg.de)

Abstract. The late Pliocene/early Pleistocene intensification of Northern Hemisphere Glaciation (iNHG) ~2.5 million years ago (Marine Isotope Stages [MIS] 100–96) stands out as an important tipping point in Earth's climate history. It strongly influenced oceanographic and climatic patterns including trade-wind and upwelling strength in the Eastern Equatorial Pacific (EEP). The thermocline depth in the EEP, in turn, plays a pivotal role for the Earth's climate system: Small changes in its depth associated with short-term climate phenomena such as the El Niño-Southern Oscillation can affect surface-water properties and therefore the ocean-atmosphere exchange. However, thermocline dynamics in the EEP during the iNHG have yet remained unclear. While numerous studies have suggested a link between a thermocline shoaling in the EEP and Northern Hemisphere ice growth, other studies have indicated a stable thermocline depth during iNHG, thereby excluding a causal relationship between thermocline dynamics and ice-sheet growth. In light of these contradictory views, we have generated geochemical (planktic foraminiferal $\delta^{18}O$, $\delta^{13}C$ and Mg/Ca), sedimentological (sand-accumulation rates) and faunal (abundance data of thermocline-dwelling foraminifera) records for Ocean Drilling Program Site 849 located in the central part of the EEP. Our records span the interval from ~2.75 to 2.4 Ma (MIS G7–95), which is critical for understanding thermocline dynamics during the final phase of the iNHG. Our new records document a thermocline shoaling from ~2.64 to 2.55 Ma (MIS G2–101) and a relatively shallow thermocline from ~2.55 Ma onwards (MIS 101–95). This indicates a state change in thermocline depth at Site 849 shortly before the final phase of iNHG. Ultimately, our data support the hypothesis that (sub-)tropical thermocline shoaling may have contributed to the development of large Northern Hemisphere ice sheets.

1 Introduction

The onset and intensification of Northern Hemisphere Glaciation during the late Pliocene and early Pleistocene (~3.6–2.4 Ma [Mudelsee and Raymo, 2005]) is part of a long-term cooling trend following the Mid-Piacenzian warm period. The glacial corresponding to Marine Isotope Stage (MIS) G6 (~2.7 Ma) is often considered to mark the onset of large-scale glaciation in the Northern Hemisphere because it is characterized by the first occurrence of ice-rafted debris in the North

Kim Jakob 6.4.18 12:16
Gelöscht: , 69120

Kim Jakob 6.4.18 12:16
Gelöscht: 60438,

Kim Jakob 6.4.18 12:16
Gelöscht: the most recent major

Kim Jakob 6.4.18 12:16
Formatiert: Englisch (USA)

Kim Jakob 6.4.18 12:16
Gelöscht: the evolution of

Kim Jakob 6.4.18 12:16
Gelöscht: ,

Kim Jakob 6.4.18 12:16
Gelöscht: thus bears important consequences for the Earth's climate system.

Kim Jakob 6.4.18 12:16
Gelöscht: to

Kim Jakob 6.4.18 12:16
Gelöscht: They

Kim Jakob 6.4.18 12:16
Gelöscht: EEP

Kim Jakob 6.4.18 12:16
Formatiert: Schriftfarbe: Automatisch

Atlantic Ocean (Bartoli et al., 2006; Bailey et al., 2013). The first culmination in Northern Hemisphere ice build-up occurred at ~2.5 Ma as documented by the first three large-amplitude (~1 ‰ in the benthic $\delta^{18}O$ record) glacial-interglacial cycles (MIS 100–96) that indicate substantial waxing and waning of ice sheets (Lisiecki and Raymo, 2005). At that time, ice rafting became widespread across the North Atlantic Ocean (Shackleton et al., 1984; Naafs et al., 2013). This so-called "intensification of Northern Hemisphere Glaciation" (iNHG) represents an important tipping point in Earth's climate history. It strongly influenced oceanographic and climatic patterns worldwide, affecting, for example, the amount of biological production in the Eastern Equatorial Pacific Ocean (EEP) (Etourneau et al., 2010; Jakob et al., 2016) – a region that exerts a strong influence on the Earth's climate system through its effects on the global carbon and nutrient cycles (e.g., Schlitzer, 2004; Takahashi et al., 2009).

Within the EEP, the position of the thermocline in the water column bears important consequences for the Earth's climate system. Today, it is poised at shallow depths. As a consequence, small changes in its depth through east-west tilting regulated by short-term climate phenomena such as the El Niño-Southern Oscillation can affect surface-water properties and therefore ocean-atmosphere exchange processes (Fedorov et al., 2004; Ma et al., 2013). In general, proxy records and modeling results consistently document a long-term shoaling of the thermocline in the EEP and other (sub-)tropical upwelling regions throughout the Plio-Pleistocene (Wara et al., 2005; Fedorov et al., 2006; Steph et al., 2006a, 2010; Dekens et al., 2007; Ford et al., 2012). However, the dynamics of the thermocline in the EEP and its potential links to the iNHG have yet remained enigmatic. Some studies have inferred that thermocline depth reached a critical threshold at ~3 Ma, which allowed trade winds to deliver cool waters from below the thermocline to the surface in (sub-)tropical upwelling regions such as the EEP (Fedorov et al., 2006; Dekens et al., 2007). The timing led to the hypothesis that thermocline shoaling and the development of the EEP "cold tongue" (Wyrtki, 1981) was a necessary precondition for iNHG through reducing poleward atmospheric heat transport (Cane and Molnar, 2001). Other studies, however, identified fundamental shifts in thermocline depth only prior to ~3.5 Ma (Wara et al., 2005; Steph et al., 2006a, 2010; Ford et al., 2012), which would imply that thermocline depth in the EEP did not play an important role in the development of large-scale glaciation in the Northern Hemisphere. In light of these contradictory views, and to ultimately shed new light on potential links between low-latitude thermocline dynamics and high-latitude ice-sheet build-up, we have investigated thermocline state changes for Ocean Drilling Program (ODP) Site 849 in the EEP during the final phase of the late Pliocene/early Pleistocene iNHG (~2.75 to 2.4 Ma, MIS G7–95).

2 Study area and study site

2.1 The Eastern Equatorial Pacific

The EEP has considerable relevance for the Earth's atmospheric and marine carbon budget (Toggweiler and Sarmiento, 1985; Takahashi et al., 2009), and at the same time exerts strong control on oceanographic and climatic circulation patterns (Fedorov and Philander, 2000; Pennington et al., 2006). Today, as a part of the tropical Pacific Walker Circulation,

Kim Jakob 6.4.18 12:16
Gelöscht: the most recent major

Kim Jakob 6.4.18 12:16
Gelöscht: Today,

Kim Jakob 6.4.18 12:16
Gelöscht: shallow depth

Kim Jakob 6.4.18 12:16
Gelöscht: EEP plays a pivotal role in the evolution of

Kim Jakob 6.4.18 12:16
Gelöscht: including

Kim Jakob 6.4.18 12:16
Gelöscht: Its position in the water column thus bears important consequences for the Earth's climate system.

Kim Jakob 6.4.18 12:16
Gelöscht: Steph et al., 2010;

Kim Jakob 6.4.18 12:16
Gelöscht: "

Kim Jakob 6.4.18 12:16
Gelöscht: via a strengthening of the tropical Pacific Walker Circulation and, at the same time, a reduction of

Kim Jakob 6.4.18 12:16
Gelöscht: . ... [1]

Kim Jakob 6.4.18 12:16
Gelöscht: during the iNHG in the EEP by integrating new with previously published proxy records from

Kim Jakob 6.4.18 12:16
Gelöscht: (Fig. 1). We use planktic (both sea-surface- and thermocline-dwelling) foraminiferal geochemical ($\delta^{18}O$, $\delta^{13}C$ and Mg/Ca) proxy records in combination with sedimentological (sand-accumulation rates) and faunal (abundance data of thermocline-dwelling foraminiferal species) information to reconstruct thermocline depth for the

Kim Jakob 6.4.18 12:16
Gelöscht: from ~

Kim Jakob 6.4.18 12:16
Gelöscht: (

Kim Jakob 6.4.18 12:16
Formatiert: Schriftfarbe: Automatisch

westward-blowing trade winds induce a year-around upwelling of cold waters from below the thermocline to the surface in the EEP. This results in a thin, nutrient-enriched and relatively cold (~23 °C; Locarnini et al., 2013) mixed layer, the so-called EEP "cold tongue" (Wyrtki, 1981) (Fig. 1b). In today's oceans, this upwelling system supports more than 10 % of the global biological production (Pennington et al., 2006). Relatively high primary productivity rates result in exceptionally high sedimentation rates that amount to up to 3.0 cm kyr^{-1} during the past 5 Myr (Mayer et al., 1992; Mix et al., 1995).

The EEP stands out as an ideal natural laboratory for studying the dynamics of the tropical thermocline: Owing to the shallow depth of the thermocline in the present-day EEP upwelling system (~50 m; Wang et al., 2000) (Fig. 1c) even small changes in its depth can affect surface-water properties such as temperature or nutrient content that can be ideally reconstructed from sediments underneath the "cold tongue". Thereby, the high sedimentation rates allow for the acquisition of proxy records at high temporal resolution compared to outside the EEP upwelling zone.

2.2 ODP Site 849

To reconstruct changes in thermocline depth in the EEP we focused on sediments from ODP Leg 138 Site 849 (coordinates: 0°11′N, 110°31′W; present-day water depth: 3851 m; Mayer et al., 1992) (Fig. 1a, b). This site has been selected because of (i) its position within the equatorial "cold tongue" west of the East Pacific Rise in the open ocean that makes it less prone to continental influence compared to sites east of the East Pacific Rise (Mix et al., 1995); (ii) the good preservation of foraminifera (Jakob et al., 2016, 2017) despite the fact that the present-day water depth at Site 849 is close to the lysocline (Adelseck and Anderson, 1978; Berger et al., 1982); and (iii) high sedimentation rates (2.7 cm kyr^{-1} for our study interval; Jakob et al., 2017) with continuous sedimentation (Mayer et al., 1992).

3 Investigated foraminiferal species

The geochemical and faunal records generated in this study (for details see Section 4) are based on the planktic foraminiferal species *Globigerinoides ruber* (white, sensu stricto), *Globorotalia crassaformis*, *Globorotalia menardii*, and *Globorotalia tumida*. the presumed calcification depths of these species in the EEP as briefly elaborated upon in the following are compiled in Figure 1c. *Globigerinoides ruber* generally inhabits and calcifies in the mixed layer and is therefore typically considered to represent surface-water conditions (Fairbanks et al., 1982; Wang, 2000; Dekens et al., 2002; Steph et al., 2009, and references therein). The species *G. menardii* and *G. tumida* are found in the EEP at depths of ~25–70 m and ~50–125 m, respectively, typically in intermediate-thermocline waters (Fairbanks et al., 1982; Watkins et al., 1998; Faul et al., 2000). *Globorotalia crassaformis* inhabits the bottom of the thermocline (Niebler et al., 1999; Regenberg et al., 2009, Steph et al., 2009, and references therein) with a rather constant calcification depth as opposed to other deep-dwelling foraminiferal species (Cléroux and Lynch-Stieglitz, 2010). Although its exact calcification depth in the EEP has remained unclear, $\delta^{18}O$ values of *G. crassaformis* from the (sub-)tropical Atlantic and the Caribbean Sea suggest that this species typically calcifies between ~400 and 800 m water depth (Steph et al., 2006b, 2009; Regenberg et al., 2009; Cléroux et al., 2013).

Kim Jakob 6.4.18 12:16
Gelöscht: in the EEP …nduce a year-arour ... [2]

Kim Jakob 6.4.18 12:16
Gelöscht: [… Wang et al., 2000])… (Fig. ... [3]

Kim Jakob 6.4.18 12:16
Gelöscht: [… Mayer et al., 1992])… (Fig. ... [4]

Kim Jakob 6.4.18 12:16
Formatiert: Schriftfarbe: Automatisch

Kim Jakob 6.4.18 12:16
Gelöscht: …. the presumed calcification d ... [5]

4 Material and methods

To reconstruct thermocline depth for the final phase of the late Pliocene/early Pleistocene iNHG from ~2.75 to 2.4 Ma (MIS G7–95), we integrate new with previously published proxy records from ODP Site 849 (Fig. 1; Tab. 1). In particular, we combine planktic (both sea-surface- and thermocline-dwelling) foraminiferal geochemical ($\delta^{18}O$, $\delta^{13}C$ and Mg/Ca) proxy records with sedimentological (sand-accumulation rates) and faunal (abundance data of thermocline-dwelling foraminiferal species) information.

4.1 Sample material

To obtain geochemical, faunal and sedimentological information for Site 849, 374 samples have been investigated along the primary shipboard splice (Mayer et al., 1992) from cores 849C-7H-1-80 cm to 849C-7H-2-21 cm and 849D-6H-5-102 cm to 849D-7H-5-57 cm (77.02–67.78 m composite depth [mcd]). Based on the age model of Jakob et al. (2017), this interval spans from ~2.75 to 2.4 Ma (MIS G7–95). Samples with a volume of 20 cm^3 were investigated at 2 cm intervals, which yields a temporal resolution of ~750 yr. The sample material was dried, weighed, and washed over a 63 µm sieve.

Foraminiferal geochemical records ($\delta^{18}O$, $\delta^{13}C$ and Mg/Ca) of the deep-thermocline-dwelling species *G. crassaformis* and the surface-dwelling species *G. ruber*, as well as sand-accumulation rates were generated from the full sample set (temporal resolution: ~750 yr). From these measurements surface-to-thermocline $\delta^{18}O$, $\delta^{13}C$ and Mg/Ca gradients were calculated. Abundance counts of both deep-thermocline- (*G. crassaformis*) and intermediate-thermocline-dwelling species (*G. menardii* and *G. tumida*) were conducted every 20 cm (temporal resolution: ~7.5 kyr).

For *G. crassaformis*, we have generated new $\delta^{18}O$, $\delta^{13}C$ and Mg/Ca records, except for the interval from ~2.65 to 2.4 Ma for which $\delta^{13}C$ values have already been published by Jakob et al. (2016). For this purpose, an average of 15 individuals per sample was picked from the 315–400 µm fraction. This size fraction has been selected to keep ontogenetic effects as small as possible (Elderfield et al., 2002; Friedrich et al., 2012) but at the same time to allow for a sufficient number of *G. crassaformis* tests per sample. Moreover, the 315–400 µm fraction ensures highest comparability to previous geochemical records of this species (e.g., Karas et al., 2009; Jakob et al., 2016). Tests for $\delta^{18}O$ and Mg/Ca analyses were cracked, homogenized and split into two subsamples. For *G. crassaformis*, both sinistral- and dextral-coiling specimens occur at Site 849; geochemical data were preferentially measured on tests with the most abundant coiling direction (sinistral). Sinistral-coiling specimens, however, do not occur continuously across our study interval. Thus, dextral-coiling tests were used for some intervals (in particular from ~2.46 to 2.43 Ma [69.84–69.04 mcd] and from ~2.51 to 2.50 Ma [70.85–70.68 mcd]). The occurrence of dextral- *versus* sinistral-coiling *G. crassaformis* specimens is random rather than following a specific cyclicity. Separate measurements of geochemical parameters ($\delta^{13}C$, $\delta^{18}O$, Mg/Ca) on sinistral- and dextral-coiling specimens from the same samples have demonstrated that the reconstructed values are independent of the coiling directions (see also Jakob et al., 2016).

Kim Jakob 6.4.18 12:16
Formatiert: Schriftfarbe: Automatisch

Kim Jakob 6.4.18 12:16
Formatiert: Schriftfarbe: Automatisch, Englisch (USA)

Kim Jakob 6.4.18 12:16
Gelöscht: Measurements

Kim Jakob 6.4.18 12:16
Gelöscht: separately

Kim Jakob 6.4.18 12:16
Gelöscht: . [

Kim Jakob 6.4.18 12:16
Gelöscht:]).

The number of *G. crassaformis* individuals in the investigated size fraction (315–400 µm), was, however, too low to allow for geochemical analyses in specific intervals. These intervals are from 2.68 to 2.65 Ma (75.39–74.65 mcd corresponding to MIS G3) and from 2.73 to 2.69 Ma (77.02–75.79 mcd corresponding to MIS G7–G5). We decided not to fill these gaps by using another size fraction because (i) this might have biased our Mg/Ca and stable-isotope records due to ontogenetic effects (Elderfield et al., 2002; Friedrich et al., 2012), and (ii) the abundance of *G. crassaformis* specimens <315 µm was also too low for geochemical analyses in most of the samples where the 315–400 µm *G. crassaformis* size fraction is absent (see Section 5.4.2 for details).

For *G. ruber*, the previously published Mg/Ca-based sea-surface temperature (SST) and $\delta^{18}O$ datasets of Jakob et al. (2017) were augmented by $\delta^{13}C$ data, except for the interval from ~2.65 to 2.4 Ma for which $\delta^{13}C$ values have already been published by Jakob et al. (2016). For this purpose, an average of twelve specimens was picked from the 250–315 µm size fraction (i.e., the fraction also used in Jakob et al., 2016). An overview of all geochemical datasets evaluated in this study is presented in Table 1.

Kim Jakob 6.4.18 12:16
Gelöscht: Sect.

Kim Jakob 6.4.18 12:16
Gelöscht: .

4.2 Analytical methods

4.2.1 Foraminiferal preservation

The preservation of planktic foraminiferal (*G. crassaformis* and *G. ruber*) tests used for geochemical analyses was examined by Scanning Electron Microscope (SEM) images of selected specimens from both glacial and interglacial intervals. Close-up views were taken using a LEO 440 SEM at the Institute of Earth Sciences, Heidelberg University.

4.2.2 Stable-isotope analyses

Oxygen and carbon isotopes of *G. ruber* and *G. crassaformis* were analyzed using a ThermoFinnigan MAT253 gas-source mass spectrometer equipped with a Gas Bench II at the Institute of Geosciences, Goethe-University Frankfurt. Values are reported relative to the Vienna Pee Dee Belemnite (VPDB) standard through the analysis of an in-house standard calibrated to NBS-19. The precision of the $\delta^{18}O$ and $\delta^{13}C$ analyses is better than 0.08 ‰ and 0.06 ‰ (at 1σ level), respectively. $\delta^{13}C$ values of *G. ruber* reported herein have been adjusted for species-specific offset from equilibrium precipitation by the addition of + 0.94 ‰ (Spero et al., 2003), while measured $\delta^{18}O$ values of *G. ruber* have been considered to approximate equilibrium precipitation (Koutavas and Lynch-Stieglitz, 2003) and therefore were not adjusted. For *G. crassaformis* we report the values measured on this species because laboratory investigations on $\delta^{13}C$ and $\delta^{18}O$ fractionation for *G. crassaformis* are still lacking.

4.2.3 Mg/Ca analyses

Samples for Mg/Ca analyses of *G. crassaformis* were carefully cleaned to remove clay minerals, organic material and re-adsorbed contaminants following the protocol of Barker et al. (2003) but omitting reductive cleaning. For selected samples,

Kim Jakob 6.4.18 12:16
Gelöscht: (2003).

however, also reductive cleaning has been applied (see Section 5.2); as a reductive reagent a mixture of hydrazine, ammonium hydroxide and ammonium citrate was used. Analyses were carried out with an Agilent Inductively Coupled Plasma-Optical Emission Spectrometer 720 at the Institute of Earth Sciences, Heidelberg University. Reported Mg/Ca values were normalized relative to the ECRM 752-1 standard reference value of 3.762 mmol/mol (Greaves et al., 2008). To ensure instrumental precision, an internal consistency standard was monitored at least every 20 samples. Based on replicate measurements, a standard deviation for Mg/Ca of ± 0.02 mmol/mol (corresponding to ± 0.12 °C) is obtained. To identify possible contamination by clay particles or diagenetic coatings that might affect foraminiferal Mg/Ca ratios (Barker et al., 2003), elemental ratios of Al/Ca, Fe/Ca and Mn/Ca were screened (see Section 5.2).

4.2.4 Paleotemperature reconstruction

Species-specific conversions of Mg/Ca to temperature for *G. crassaformis* have only been calibrated based on samples from the Atlantic Ocean (Anand et al., 2003; Regenberg et al., 2009; Cléroux et al., 2013). These equations yield the same trend and amplitudes when applied to *G. crassaformis* Mg/Ca values from Site 849, but differ with regard to absolute values (Fig. 2). We converted Mg/Ca ratios of *G. crassaformis* into temperature following the species-specific equation of Cléroux et al. (2013) for two reasons: (i) The selected calibration is based on specimens with a grain size of 355–425 µm, which matches the size fraction used in our study (315–400 µm) better than the other equations that are available; and (ii) the Mg/Ca range of *G. crassaformis* from Site 849 (~1–3 mmol/mol) fits best to the calibration range (~1–2 mmol/mol) of the equation of Cléroux et al. (2013) compared to the other equations.

Because the equation of Cléroux et al. (2013) is based on oxidative and reductive cleaning of foraminiferal tests, while only oxidative cleaning has been applied to Site 849 samples, measured Mg/Ca values had to be reduced by 10 % (Barker et al., 2003). The pooled uncertainty in the temperature record is ± 0.94 °C (analytical error of ± 0.02 mmol/mol [corresponding to ± 0.12 °C] and calibrational error of ± 0.82 °C [Cléroux et al., 2013]).

4.2.5 Abundance counts

Following the approach of Sexton and Norris (2008), abundance counts of deep-thermocline-dwelling (*G. crassaformis,* both sinistral- and dextral-coiling specimens) and intermediate-thermocline-dwelling (*G. tumida* and *G. menardii*) species (Fig. 1c) were generated on the >250 µm size fraction of Site 849 samples. The >250 µm size fraction was split down to at least 400 individual planktic foraminifera using a microsplitter. Abundance counts were converted to mass-accumulation rates using linear sedimentation rates and dry bulk density data (calculated from high-resolution GRAPE density shipboard measurements [IODP JANUS database; Mayer et al., 1992]) following the methodology described in Jakob et al. (2016).

4.2.6 Sand-accumulation rates

The sand-accumulation rates available for the MIS G1–95 (~2.65–2.4 Ma) interval from Site 849 as presented in Jakob et al. (2016) were extended back to MIS G7 (~2.75 Ma) in this study. They were calculated using linear sedimentation rates, dry

Kim Jakob 6.4.18 12:16
Gelöscht: Sect.

Kim Jakob 6.4.18 12:16
Gelöscht:]) is ± 0.94 °C.

Kim Jakob 6.4.18 12:16
Gelöscht: Abundance

Kim Jakob 6.4.18 12:16
Gelöscht: 1b

Kim Jakob 6.4.18 12:16
Gelöscht: (SAR)

bulk density data (calculated from high-resolution GRAPE density shipboard measurements [IODP JANUS database; Mayer et al., 1992]), and the portion of the >63 µm sand fraction following the approach described in Jakob et al. (2016).

5 Results and discussion

5.1 Foraminiferal test preservation at Site 849

Shipboard investigations on core catchers had originally reported a poor preservation of planktic foraminiferal tests at Site 849 (Mayer et al., 1992). However, these observations do not apply to the samples from our study interval. Instead, SEM images of both glacial and interglacial *G. crassaformis* and *G. ruber* specimens consistently show well-preserved fine features such as delicate spines, pore channels and a layered wall structure, and a lack of secondary calcite or crusts on test surfaces (Fig. 3). This indicates that test preservation is consistently sufficient for the acquisition of high-quality geochemical data for both species throughout the study interval. A low planktic foraminiferal fragmentation index (Jakob et al., 2017) together with large numbers of well-preserved, although typically less resistant specimens such as *Globigerinoides* (Dittert et al., 1999) (Fig. 3g–l) further confirms this interpretation, indicating that dissolution has not considerably affected foraminiferal tests.

5.2 Assessment of contamination and diagenetic effects on Mg/Ca ratios of *G. crassaformis*

Al/Ca, Fe/Ca and Mn/Ca ratios >0.1 mmol/mol are typically considered to indicate the presence of detrital clay, Fe-rich coatings and Mn-rich overgrowth, respectively, and therefore hint at foraminiferal test contamination that might have biased measured Mg/Ca ratios (Barker et al., 2003). In most of our samples the content of Al was below the detection limit, arguing against the presence of detrital clay. With the exception of few samples, Fe/Ca values also commonly do not exceed the critical value of 0.1 mmol/mol and therefore indicate no contamination by Fe-rich overgrowth (Fig. 4a). The lack of a statistically significant correlation between Mg/Ca and Fe/Ca ratios ($r^2 = 0.17$, $p < 0.01$) further supports this finding.

Measured Mn/Ca ratios, however, were above the 0.1 mmol/mol threshold and therefore might indicate Mn-rich overgrowth on the analyzed tests (Fig. 4b). Reductive cleaning (in addition to the standard cleaning procedure applied to Site 849 samples; see Section 4.2.3) performed on selected samples shows by ~40–45 % lower Mn/Ca values compared to values derived from oxidative cleaning only. This indicates at least two different Mn phases coexisting on *G. crassaformis* test surfaces. A similar observation has been made for the thermocline-dwelling species *Neogloboquadrina dutertrei* from nearby ODP Site 1240 located in the Panama Basin. In this study, Mn-rich phases not removed through oxidative cleaning are hypothesized to arise from "kutnahorite-like" carbonates or Mn-oxyhydroxide (Pena et al., 2005) – Mn phases perhaps also existing on *G. crassaformis* test surfaces at Site 849. Indeed, our data show a weak correlation between Mg/Ca and Mn/Ca ratios for *G. crassaformis* samples ($r^2 = 0.44$, $p < 0.01$) that might indicate a bias of measured Mg/Ca ratios due to a Mn-rich overgrowth. We note, however, that SEM images argue against the existence of any kind of overgrowth (Fig. 3). Diagenetic overgrowth usually has a Mg/Mn ratio of ~0.1 mol/mol (Barker et al., 2003, and references therein). If an

Kim Jakob 6.4.18 12:16
Formatiert: Schriftfarbe: Automatisch

Kim Jakob 6.4.18 12:16
Gelöscht: at Site 849

Kim Jakob 6.4.18 12:16
Gelöscht: (Jakob et al., 2017),

Kim Jakob 6.4.18 12:16
Gelöscht: Our

Kim Jakob 6.4.18 12:16
Gelöscht: indeed

Kim Jakob 6.4.18 12:16
Gelöscht: . ... [6]

unrealistically high Mg/Mn ratio of 1 in the diagenetic overgrowth is assumed, this might change temperature estimates by on average ~0.5 °C; however, we note that this would not affect the overall shape of the Mg/Ca-based temperature record (Fig. 4c, d). We therefore conclude with reasonable certainty that early diagenetic overprinting has no significant impact on the interpretation of our data, although we cannot rule out the possibility of diagenetic changes in *G. crassaformis* tests because of significantly enriched Mn/Ca ratios.

5.3 Geochemical records of *G. crassaformis* and *G. ruber* at Site 849

In warm tropical waters, where seasonal climate variability is low, geochemical signatures of the investigated foraminiferal species are typically considered not to be seasonally biased (Lin et al., 1997; Tedesco et al., 2007; Mohtadi et al., 2009; Jonkers and Kučera, 2015). At Site 849, seasonal temperature variability is presently ~0.4 °C (i.e., SST of ~24 °C during summer [June] *versus* ~23.6 °C during winter [January]). The same seasonal amplitude (~0.4 °C) prevails at 20 m water depth (Locarnini et al., 2013), i.e., the assumed mean depth habitat of the here investigated species *G. ruber* (Wang, 2000; see also Section 3). Further, we suggest seasonality to decrease with increasing water depth and therefore to be <0.4 °C at the calcification depth of *G. crassaformis*. Thus, because of the low seasonal temperature variability, it is reasonable to assume that all geochemical data derived from Site 849 (Figs. 5–8) reflect mean annual conditions.

5.3.1 Stable-isotope data

The $\delta^{18}O$ record of *G. crassaformis* varies between 0.91 ‰ and 2.79 ‰ throughout the study interval (~2.75–2.4 Ma) (Fig. 5b). Lowest values correspond to interglacials and highest values are associated with glacials. With a mean value of 2.01 ‰, $\delta^{18}O$ values of *G. crassaformis* (this study) are on average 2.78 ‰ higher than those of *G. ruber* (Jakob et al., 2017), indicating cooler and/or more saline waters at the calcification depth of *G. crassaformis* (bottom of the thermocline) compared to that of *G. ruber* (surface waters) (Fig. 1c; see Section 3 for details). In theory, a deeper calcification depth of *G. crassaformis* than of *G. ruber* should result in a lower $\delta^{13}C$ signature in *G. crassaformis* tests than in those from *G. ruber* since the amount of organic matter remineralization and the associated release of light ^{12}C into the surrounding water typically increases with water depth (Deuser and Hunt, 1969; Kroopnick, 1985). Indeed, by ~1.86 ‰ lower $\delta^{13}C$ values are recorded for *G. crassaformis* (mean: 0.46 ‰) than for *G. ruber* (mean: 2.32 ‰; Jakob et al., 2016; this study) (Fig. 5c). In general, $\delta^{13}C$ values of *G. ruber* and *G. crassaformis* fluctuate between minima of 1.36 ‰ and 0 ‰ during glacials and maxima of 2.97 ‰ and 0.97 ‰ during interglacials, respectively (Jakob et al., 2016; this study) (Fig. 5c). It has been shown in a former study that the glacial-interglacial foraminiferal $\delta^{13}C$ pattern at Site 849 during iNHG is strongly controlled by the amount of primary productivity in the Southern Ocean, which is highest during interglacials (high $\delta^{13}C$) and lowest during glacials (low $\delta^{13}C$) (Jakob et al., 2016).

Kim Jakob 6.4.18 12:16
Gelöscht: Although we cannot completely rule out the possibility of diagenetic changes in the *G. crassaformis* tests because of significantly enriched Mn/Ca ratios, we

Kim Jakob 6.4.18 12:16
Gelöscht: (if existing)

Kim Jakob 6.4.18 12:16
Formatiert: Durchstreichen

Kim Jakob 6.4.18 12:16
Gelöscht: Stable-isotope and Mg/Ca

Kim Jakob 6.4.18 12:16
Gelöscht: the tropics

Kim Jakob 6.4.18 12:16
Gelöscht:). Therefore, all data presented in this study are inferred to

Kim Jakob 6.4.18 12:16
Formatiert: Schriftart:Nicht Fett

Kim Jakob 6.4.18 12:16
Gelöscht: .

Kim Jakob 6.4.18 12:16
Gelöscht: in

Kim Jakob 6.4.18 12:16
Gelöscht: habitat

Kim Jakob 6.4.18 12:16
Gelöscht: 1b

Kim Jakob 6.4.18 12:16
Gelöscht: Sect.

Kim Jakob 6.4.18 12:16
Gelöscht: habitat

Kim Jakob 6.4.18 12:16
Gelöscht: ‰) (

5.3.2 Mg/Ca-based temperature data

Mg/Ca values of *G. crassaformis* vary between 0.82 mmol/mol and 3.02 mmol/mol (this study), being on average 1.43 mmol/mol lower than Mg/Ca ratios of *G. ruber* from the same site and time interval (Jakob et al., 2017) (Fig. 5d). Temperatures reconstructed from *G. crassaformis* Mg/Ca values cover a range from 1.0 °C to 11.6 °C. Thus, sub-thermocline temperatures at Site 849 derived from *G. crassaformis* are on average 19 °C lower than SSTs as reflected by *G. ruber* (~22–27 °C; Jakob et al., 2017) (Fig. 5d). To bring *G. crassaformis*-based temperatures of this study into a broader temporal and geographical context we next compare this record to a number of other relevant datasets:

(i) The temperature range reconstructed based on *G. crassaformis* at Site 849 is close to temperatures inferred for the same species and time interval at Deep Sea Drilling Project (DSDP) Site 214 in the tropical eastern Indian Ocean (~8–10 °C; Karas et al., 2009) (Figs. 1a, 6b). Yet available Mg/Ca-based thermocline-temperature records from the east Pacific for the ~2.75–2.4 Ma interval capture ranges of ~17–22.5 °C (ODP Site 1241, *G. tumida*-based; Steph et al., 2006a), ~18–21 °C (Site 1241, *N. dutertrei*-based; Groeneveld et al., 2014) and ~15.5–17.5 °C (Site 849, *G. tumida*-based; Ford et al., 2012) (Figs. 1a, b and 6b, c). In comparison to thermocline temperature records from Site 1241 (Steph et al., 2006a; Groeneveld et al., 2014) our new *G. crassaformis*-based temperatures appear to be relatively low. However, this discrepancy can likely be explained with different calcification depths of the investigated species (and therefore different temperatures reflected; Cléroux et al., 2013) together with differences in the oceanographic setting of the investigated sites (i.e., Site 849 in the "cold tongue" *versus* Site 1241 in the "warm pool" with, for example, a modern-day SST difference of ~3 °C; Locarnini et al., 2013; see also Section 5.4.1). The record from Site 849 by Ford et al. (2012) is of low temporal resolution with only six datapoints across our study interval such that peak (both glacial and interglacial) temperatures are probably not captured. A comparison to this record is therefore not robust enough to warrant further discussion.

(ii) The EEP upwelling system is mainly fed by waters derived from the Southern Ocean (e.g., Tsuchiya et al., 1989). However, relatively warm SSTs in the Southern Ocean during our study interval (~10.5–17 °C at ODP Site 1090 [Martínez-Garcia et al., 2010; Fig. 1a] – a site accepted as the best endmember of Southern Ocean waters [Billups et al., 2002; Pusz et al., 2011]) are difficult to reconcile with substantially lower temperatures recorded in thermocline waters at EEP Site 849 (~1–11.6 °C; this study) and Indian Ocean Site 214 (~8–10 °C; Karas et al., 2009). Together, these datasets imply strong cooling of Southern Ocean surface waters either when being downwelled and transported to the lower latitudes and/or through mixing with cold (presently ~0 °C; Craig and Gordon, 1965) Antarctic Bottom Waters.

(iii) Thermocline temperatures of the Last Glacial Maximum are expected to be substantially colder than those of the Plio-/Pleistocene transition (Ford et al., 2012). However, in comparison to tropical east Pacific thermocline temperatures of the Last Glacial Maximum (on average ~14–16 °C) that derive from Mg/Ca data of *G. tumida* from Site 849 (Ford et al., 2015) and *N. dutertrei* from Sites 08JC and 17JC (Hertzberg et al., 2016) (Fig. 1a) deep-thermocline temperatures of *G. crassaformis* at Site 849 from the ~2.75–2.4 Ma interval appear to be too low. We suggest that different calcification depths of the investigated species may explain this discrepancy (Cléroux et al., 2013).

Kim Jakob 6.4.18 12:16
Gelöscht: .

Kim Jakob 6.4.18 12:16
Gelöscht: sea-surface temperatures

Kim Jakob 6.4.18 12:16
Gelöscht: [

Kim Jakob 6.4.18 12:16
Gelöscht:])

(iv) Finally, we notice that modern bottom-water temperatures at our study site of ~1.5 °C (Locarnini et al., 2013) overlap the deep-thermocline temperature range as reconstructed from *G. crassaformis*-based Mg/Ca data. Very low *G. crassaformis*-based temperatures of ~1 °C derive, however, from a single datapoint, while temperatures typically higher than 2–3 °C even during prominent iNHG glacials can be reconciled better with present-day bottom-water temperatures.

5.4 Thermocline development in the Eastern Equatorial Pacific

5.4.1 Geochemical evidence

Variations in the vertical temperature gradient within the upper water column allow to effectively monitor shifts in thermocline depth with a small temperature difference between surface and thermocline waters indicating a deep thermocline and *vice versa* (e.g., Steph et al., 2009; Nürnberg et al., 2015). Absolute values of surface-to-thermocline temperature gradients can be reconstructed from the Mg/Ca-based temperature gradient derived from surface-dwelling and thermocline-dwelling species. In addition, the $\delta^{18}O$ gradient provides information on relative changes in the surface-to-thermocline temperature gradient (as opposed to absolute estimates derived from the Mg/Ca-gradient). This is because salinity might also play a role in controlling $\delta^{18}O$ values of foraminifera inhabiting different depths. The effect of global ice volume (i.e., the third factor beside temperature and salinity that affect foraminiferal $\delta^{18}O$; Ravelo and Hillaire-Marcel, 2007) should be identical. For gradient calculations the species *G. ruber* is ideally suited as a surface-water recorder since it is one of the shallowest-dwelling species among modern planktic foraminifera (Bé, 1977), while *G. crassaformis* appears to be one of the most promising recorder of the deep thermocline because of its rather constant calcification depth compared to other deep dwellers (Cléroux and Lynch-Stieglitz, 2010). This approach (i.e., *G. ruber* to *G. crassaformis* gradient calculation) has already successfully been applied by previous studies that have investigated changes in surface-water structure and thermocline through time (e.g., Karas et al., 2009; Bahr et al., 2011).

The $\delta^{18}O$- and Mg/Ca-based temperature gradients between *G. ruber* and *G. crassaformis* at Site 849 show no glacial-interglacial cyclicity (Fig. 7b), indicating that thermocline depth was unaffected by varying glacial *versus* interglacial climatic conditions. This observation is in line with previous modeling efforts (Lee and Poulsen, 2005) and proxy-based (both geochemical and faunal) studies from EEP "cold tongue" ODP Sites 846 and 849 that cover the same time interval (Bolton et al., 2010; Jakob et al., 2017). However, it contradicts geochemical data (i.e., the surface-to-thermocline [*Globigerinoides sacculifer* to *N. dutertrei*] Mg/Ca-based temperature gradient) derived from Site 1241 located in the east Pacific "warm pool" that shows glacial-interglacial variations in thermocline depth for MIS 100–96 (Groeneveld et al., 2014) (Fig. 8b). Therefore, we hypothesize that thermocline depth underwent a different evolution on the glacial-interglacial timescale in regions inside (Sites 846 and 849) and outside (Site 1241) the "cold tongue". Further, water-column stratification and therefore thermocline depth at Site 1241 has been shown to be affected by glacioeustatic closures of the Central American Seaway that temporally occurred during MIS 100–96 (Groeneveld et al., 2014), perhaps through upwelling intensification (Schneider and Schmittner, 2006). In contrast, Site 849 appears to be unaffected by such changes as

Kim Jakob 6.4.18 12:16
Formatiert: Schriftart:Kursiv

Kim Jakob 6.4.18 12:16
Gelöscht: (e.g., *G. ruber*)

Kim Jakob 6.4.18 12:16
Gelöscht: (e.g., *G. crassaformis*)

Kim Jakob 6.4.18 12:16
Gelöscht: of the same species

Kim Jakob 6.4.18 12:16
Gelöscht: since the

Kim Jakob 6.4.18 12:16
Gelöscht: and salinity

Kim Jakob 6.4.18 12:16
Gelöscht: two other main factors

Kim Jakob 6.4.18 12:16
Gelöscht: [

Kim Jakob 6.4.18 12:16
Gelöscht:])

Kim Jakob 6.4.18 12:16
Gelöscht: for

Kim Jakob 6.4.18 12:16
Gelöscht: species from the same locality.

Kim Jakob 6.4.18 12:16
Gelöscht: 6b

Kim Jakob 6.4.18 12:16
Gelöscht: in the EEP

Kim Jakob 6.4.18 12:16
Gelöscht: vs.

Kim Jakob 6.4.18 12:16
Gelöscht: model-

shown by sand-accumulation-rate-based data on export production (Jakob et al., 2016). Hence it is likely that Site 1241 reflects a more local signal as opposed to an open-ocean, quasi-global signal reported at Site 849 due to its position west of the East Pacific Rise (Mix et al., 1995).

On longer timescales, the $\delta^{18}O$ gradient at Site 849 decreased by ~1 ‰ from ~2.64 Ma to 2.55 Ma (MIS G2–101), and remained relatively constant throughout the remainder of our study interval (~2.55–2.38 Ma; MIS 101–95) (Fig. 7b). The Mg/Ca-based temperature gradient shows the same overall pattern as the $\delta^{18}O$ gradient (i.e., a ~5 °C increase from ~2.64 Ma to 2.55 Ma, and a constant value of ~20 °C from ~2.55 to 2.38 Ma) (Fig. 7b). We interpret the decrease in the $\delta^{18}O$ gradient and the increase in the Mg/Ca-based temperature gradient from ~2.64 Ma to 2.55 Ma to represent a shoaling of the thermocline. From that time onwards, constant $\delta^{18}O$ and Mg/Ca-based temperature gradients suggest that the thermocline remained relatively shallow throughout the final phase of the late Pliocene/early Pleistocene iNHG until ~2.38 Ma. In general, the shoaling trend of the thermocline revealed by our records agrees with the overall long-term shoaling trend of the thermocline in the EEP observed throughout the Plio-Pleistocene (Fedorov et al., 2006; Steph et al., 2006a, 2010; Dekens et al., 2007; Ford et al., 2012), although substantial thermocline shoaling is restricted to the ~2.64–2.55 Ma period rather than occurring continuously throughout the entire investigated time interval (Fig. 8). However, our data do not confirm previous datasets indicating that most prominent thermocline shoaling occurred prior to ~3.5 Ma (Wara et al., 2005; Steph et al., 2006a, 2010; Ford et al., 2012). Geochemical data from Site 1241 even reveal a transient thermocline deepening for the ~2.7–2.5 Ma interval (Steph et al., 2006a) (Fig. 8b), which also cannot be confirmed by our records from Site 849 and therefore supports that Site 1241 might reflect a more local signal (see above). Other records used to infer thermocline evolution in the east Pacific for this interval lack the required temporal resolution (~10–30 kyr [Wara et al., 2005; Dekens et al., 2007; Ford et al., 2012] *versus* ~0.75–3 kyr [Steph et al., 2006a; this study]) to resolve transient thermocline changes as observed at Site 1241, if existent.

Kim Jakob 6.4.18 12:16
Gelöscht: time scales

Kim Jakob 6.4.18 12:16
Gelöscht: 6b

Kim Jakob 6.4.18 12:16
Gelöscht: 6b

5.4.2 Faunal and sedimentological evidence

Based on our data, the overall abundances of the deep-thermocline-dwelling species *G. crassaformis* at Site 849 were relatively low when the thermocline was relatively deep (i.e., prior to ~2.55 Ma as indicated by the $\delta^{18}O$ and Mg/Ca-based temperature gradients) (Fig. 7c). More specifically, *G. crassaformis* was present in substantially reduced numbers only or even completely absent between ~2.73 and 2.64 Ma (MIS G7–G2; with the exception of MIS G4 [~2.69–2.68 Ma]). Since ~2.64 Ma, i.e., when the thermocline started to shoal, relative *G. crassaformis* abundances increased markedly from typically <5 % to ~10–35 % such that representatives of this taxon are present continuously throughout the remainder of the study interval. The increase of *G. crassaformis* abundances occurs at the expense of the intermediate-thermocline-dwelling species *G. menardii* and *G. tumida*, which decline from ~30–75 % to only ~5–65 % (Fig. 7c). This observation suggests that prior to the final phase of the late Pliocene/early Pleistocene iNHG, when the thermocline was relatively deep, the living conditions for the deep-thermocline-dwelling species *G. crassaformis* were unfavorable. At the same time, low *G. crassaformis* abundances allowed intermediate-thermocline-dwelling species (such as *G. menardii* and *G. tumida*) to dominate the

Kim Jakob 6.4.18 12:16
Gelöscht: in the EEP

Kim Jakob 6.4.18 12:16
Gelöscht: 6c

Kim Jakob 6.4.18 12:16
Gelöscht:) (

Kim Jakob 6.4.18 12:16
Gelöscht: 68

Kim Jakob 6.4.18 12:16
Gelöscht: 69

Kim Jakob 6.4.18 12:16
Gelöscht: 6c

planktic foraminiferal assemblages. However, we note that thermocline depth is most probably not the sole factor regulating *G. crassaformis* abundances. This is because this species reaches only low percentages within modern planktic foraminiferal assemblages in the EEP (typically <1 % in core-top samples; Prell 1985) although the present-day thermocline is relatively shallow.

In general, *G. crassaformis* reaches highest abundances in oxygen-depleted waters (Jones, 1967; Kemle von Mücke and Hemleben, 1999), while other environmental factors including temperature, salinity or nutrient availability are markedly less important (Cléroux et al., 2013). The oxygen content of deep waters (and accordingly the abundance of *G. crassaformis*) is typically closely coupled to surface-water productivity (with a lower oxygen level and higher *G. crassaformis* abundances in deeper waters when surface-water productivity is high) (Wilson et al., 2017). We therefore hypothesize that primary productivity at Site 849 prior to ~2.64 Ma (MIS G2) was relatively low (with the exception of MIS G4). Low primary productivity led to a reduction of organic matter remineralization and therefore oxygen consumption in deeper waters. An elevated oxygen content in deeper waters implies, in turn, low *G. crassaformis* abundances. Such a scenario is supported by the sand-accumulation-rate-based primary productivity record from Site 849 (Jakob et al., 2016; this study), which clearly indicates low productivity rates prior to ~2.64 Ma when the thermocline was relatively deep compared to after ~2.64 Ma when the thermocline became shallow (Fig. 7b, d).

As outlined above, on longer timescales primary productivity at Site 849 appears to be coupled to variations in thermocline depth. The observed long-term trend in primary productivity is overprinted by a clear glacial-interglacial cyclicity particularly during the final phase of iNHG (MIS 100–96); the position of the thermocline, however, remained constant along the obliquity (i.e., 41-kyr) band (Fig. 7b, d). Notably, the accumulation rates of *G. crassaformis, G. menardii* and *G. tumida* perfectly capture the pattern derived by the sand-accumulation-rate-based productivity record (Fig. 7c, d). This suggests that the abundances of deep- and intermediate-thermocline-dwelling foraminiferal species are coupled to the strength of the biological pump and can be used as a tracer for primary productivity at Site 849.

The relatively high $\delta^{13}C$ gradient for MIS G4–G2 as it emerges from our data (Fig. 7d) confirms the interpretation of Jakob et al. (2016) for MIS G1–95 that low-amplitude productivity changes prior to MIS 100 were mainly driven by the nutrient content within the upwelled water mass as long as the thermocline was relatively deep (as reflected by a low thermocline-to-surface temperature gradient prior to ~2.55 Ma [MIS 101]; Fig. 7b, d). High-amplitude productivity changes resulting from upwelling intensification played an important role from MIS 100 onward (Jakob et al., 2016). At the same time, the thermocline became relatively shallow (as reflected by a large thermocline-to-surface temperature gradient since ~2.55 Ma [MIS 101] at Site 849; Fig. 7b, d). This is unlikely a coincidence, but rather suggests that the thermocline depth reached a critical threshold at that time. Prior to this, relatively warm and nutrient-poor waters from above the thermocline have upwelled at EEP Site 849. Consequently, primary productivity rates were low. When the thermocline became shallow enough, however, trade winds could deliver cooler, nutrient-enriched waters from below the thermocline to the surface, which allowed primary productivity to increase. Such a scenario is supported by the observation that lower SSTs prevailed at Site 849 during glacials since MIS 100 (Jakob et al., 2017) (Fig. 5d). Moreover, temporal closures of the Central American

Kim Jakob 6.4.18 12:16
Gelöscht: SAR

Kim Jakob 6.4.18 12:16
Gelöscht: 6b

Kim Jakob 6.4.18 12:16
Gelöscht: 6b

Kim Jakob 6.4.18 12:16
Gelöscht: SAR

Kim Jakob 6.4.18 12:16
Gelöscht: 6c

Kim Jakob 6.4.18 12:16
Gelöscht: 6d

Kim Jakob 6.4.18 12:16
Gelöscht: 6b

Kim Jakob 6.4.18 12:16
Gelöscht: 6b

Kim Jakob 6.4.18 12:16
Gelöscht: in the

Seaway might have additionally promoted generally increasing upwelling and therefore primary productivity rates since MIS 100 (Schneider and Schmittner, 2006; Groeneveld et al., 2014).

Our findings imply a marked effect of long-term thermocline state change on primary productivity at the studied site. In particular, when thermocline shoaling reached a critical threshold, primary productivity increased, thereby removing CO_2 from the surface ocean. Thermocline shoaling appears to be a consistent feature in the EEP throughout the Plio-/Pleistocene (although the timing and magnitude varies between different studies which may be related to different approaches for thermocline reconstruction or different localities and therefore local oceanography). Considering that the entire EEP contributes substantially to global biological production in the present-day oceans (Pennington et al., 2006), the observed coupling between thermocline state change and primary productivity (if behaving similar in the entire EEP "cold tongue") is of major importance for the Earth's climate. It may have favored global cooling and therefore the early development of large ice sheets in the Northern Hemisphere. At the same time, as suggested in previous studies, the formation of the "cold tongue" through thermocline shoaling might have additionally preconditioned the iNHG by reducing atmospheric heat transport from the tropics to the poles (Cane and Molnar, 2001).

6 Conclusions

We integrate new with previously published foraminiferal-based geochemical, faunal, and sedimentological records for ODP Site 849 (~2.75–2.4 Ma, MIS G7–95) to reconstruct changes in thermocline depth during the late Pliocene/early Pleistocene iNHG. Our data document a shoaling of the thermocline at Site 849 from ~2.64 to 2.55 Ma, while it remained relatively shallow until ~2.38 Ma, implying that major changes in thermocline depth occurred shortly before the final phase of the late Pliocene/early Pleistocene iNHG (i.e., prior to MIS 100–96). This finding, which is in line with former studies (Fedorov et al., 2006; Dekens et al., 2007), supports the hypothesis that (sub-)tropical thermocline shoaling was a precondition to allow the development of large ice sheets in the Northern Hemisphere (Cane and Molnar, 2001). At the same time, our new data contradict studies that have documented substantial shifts in thermocline depth in the EEP only prior to ~3.5 Ma (Wara et al., 2005; Steph et al., 2006a, 2010; Ford et al., 2012). Our new records also suggest low primary productivity rates during times of a relatively deep thermocline prior to ~2.64 Ma (MIS G2). In turn, the relatively shallow thermocline associated with low SSTs after ~2.55 Ma allowed primary productivity to increase during prominent iNHG glacials (MIS 100–96) and, perhaps, by removing CO_2 from ocean-atmosphere exchange processes, to further stimulate Northern Hemisphere ice-sheet growth.

Data availability

All data reported will be made available upon publication of this paper via the open access PANGAEA database (www.pangaea.de).

Kim Jakob 6.4.18 12:16
Gelöscht: in

Kim Jakob 6.4.18 12:16
Gelöscht: EEP

Kim Jakob 6.4.18 12:16
Gelöscht: ,

Kim Jakob 6.4.18 12:16
Gelöscht: ; thus, it

Kim Jakob 6.4.18 12:16
Formatiert: Schriftfarbe: Automatisch

Kim Jakob 6.4.18 12:16
Gelöscht: and

Kim Jakob 6.4.18 12:16
Gelöscht: records

Kim Jakob 6.4.18 12:16
Gelöscht: with

Kim Jakob 6.4.18 12:16
Gelöscht: data

Kim Jakob 6.4.18 12:16
Gelöscht: in the EEP

Kim Jakob 6.4.18 12:16
Gelöscht: in the EEP

Kim Jakob 6.4.18 12:16
Gelöscht: a

Kim Jakob 6.4.18 12:16
Gelöscht:).

Kim Jakob 6.4.18 12:16
Formatiert: Schriftfarbe: Automatisch

Kim Jakob 6.4.18 12:16
Formatiert: Englisch (USA)

Author contributions

The project was designed by OF, KAJ, and JP. KAJ and CS carried out Mg/Ca analyses; JF and KAJ performed stable-isotope analyses. KAJ wrote the manuscript with input from all co-authors.

Competing interests

The authors declare that they have no conflict of interest.

Acknowledgments

Richard Norris provided invaluable support in foraminiferal taxonomy. Sven Hofmann and Silvia Rheinberger are thanked for stable-isotope and Mg/Ca analyses, respectively. André Bahr provided support in Mg/Ca sample preparation. Hans-Peter Meyer and Alexander Varychev provided SEM assistance. Jani L. Biber, Verena Braun, Jakob Gänzler, Barbara Hennrich, Karsten Kähler, and Tobias Syla helped with processing of sediment samples. Comments and suggestions by editor Luc Beaufort and two anonymous reviewers are highly appreciated. This research used samples provided by the Ocean Drilling Program, which was sponsored by the U.S. National Science Foundation and participating countries under the management of Joint Oceanographic Institutions, Inc. Funding for this study was provided by the German Research Foundation (DFG; grants FR2544/6 to O.F. and PR651/15 to J.P.).

References

Adelseck, C. G. and Anderson, T. F.: The late Pleistocene record of productivity fluctuations in the eastern equatorial Pacific Ocean, Geology, 6, 388–391, 1978.

Anand, P., Elderfield, H., and Conte, M. H.: Calibration of Mg/Ca thermometry in planktonic foraminifera from a sediment trap time series, Paleoceanography, 18, doi:1010.1029/2002PA000846, 2003.

Bahr, A., Nürnberg, D., Schönfeld, J., and Garbe-Schönberg, D.: Hydrological variability in Florida Straits during Marine Isotope Stage 5 cold events, Paleoceanography, 26, PA2214, doi:10.1029/2010PA002015, 2011.

Bailey, I., Hole, G. M., Foster, G. L., Wilson, P. A., Storey, C. D., Trueman, C. N., and Raymo, M. E.: An alternative suggestion for the Pliocene onset of major northern hemisphere glaciation based on the geochemical provenance of North Atlantic Ocean ice-rafted debris, Quaternary Sci. Rev., 75, 181–194, 2013.

Barker, S., Greaves, M., and Elderfield, H.: A study of cleaning procedures used for foraminiferal Mg/Ca paleothermometry, Geochem. Geophys. Geosys., 4, doi:10.1029/2003GC000559, 2003.

Kim Jakob 6.4.18 12:16
Formatiert: Schriftfarbe: Automatisch

Kim Jakob 6.4.18 12:16
Formatiert: Schriftfarbe: Automatisch

Kim Jakob 6.4.18 12:16
Gelöscht: (Scripps Institution of Oceanography, San Diego)

Kim Jakob 6.4.18 12:16
Gelöscht: (Goethe-University Frankfurt)

Kim Jakob 6.4.18 12:16
Gelöscht: (Heidelberg University)

Kim Jakob 6.4.18 12:16
Formatiert: Schriftfarbe: Automatisch

Bartoli, G., Sarnthein, M., and Weinelt, M.: Late Pliocene millennial-scale climate variability in the northern North Atlantic prior to and after the onset of Northern Hemisphere glaciation, Paleoceanography, 21, PA4205, doi:4210.1029/2005PA001185, 2006.

Bé, A. W. H.: An ecological, zoogeographic and taxonomic review of recent planktonic foraminifera, in: Oceanic micropaleontology, edited by: Ramsey, A. T. S., Academic Press, London, 1–100, 1977.

Berger, W. H., Bonneau, M.-C., and Parker, F. L.: Foraminifera on the deep-sea floor: lysocline and dissolution rate, Oceanol. Acta, 5, 249–258, 1982.

Billups, K., Channell, J. E. T., and Zachos, J.: Late Oligocene to early Miocene geochronology and paleoceanography from the subantarctic South Atlantic. Paleoceanography, 17(1), 1004, doi:10.1029/2000PA000568, 2002.

Bolton, C. T., Gibbs, S. J., and Wilson, P. A.: Evolution of nutricline dynamics in the equatorial Pacific during the late Pliocene, Paleoceanography, 25, PA1207, doi:1210.1029/2009PA001821, 2010.

Cane, M. A. and Molnar, P.: Closing of the Indonesian seaway as a precursor to east African aridification around 3–4 million years ago, Nature, 411, 157–162, 2001.

Cléroux, C., and Lynch-Stieglitz, J.: What caused G. truncatulinoides to calcify in shallower water during the early Holocene in the western Atlantic/Gulf of Mexico?, IOP Conf. Ser. Earth Environ. Sci., 9, doi:10.1088/1755-1315/9/1/012020, 2010.

Cléroux, C., deMenocal, P., Arbuszewski, J., and Linsley, B.: Reconstructing the upper water column thermal structure in the Atlantic Ocean, Paleoceanography, 28, 503–516, 2013.

Craig, H., and Gordon, L. I.: Deuterium and oxygen-18 variations in the ocean and the marine atmosphere, in: Stable isotopes in oceanographic studies and paleotemperatures, edited by: Tongiorgi, E., Spoletto, Pisa, 9–130, 1965.

Dekens, P. S., Lea, D. W., Pak, D. K., Spero, H. J.: Core top calibration of Mg/Ca in tropical foraminifera: Refining paleotemperature estimation, Geochem. Geophys. Geosys., 3, doi:10.1029/2001GC000200, 2002.

Dekens, P. S., Ravelo, A. C., and McCarthy, M. D.: Warm upwelling regions in the Pliocene warm period, Paleoceanography, 22, PA3211, doi:3210.1029/2006PA001394, 2007.

Deuser, W. G. and Hunt, J. M.: Stable isotope ratios of dissolved inorganic carbon in the Atlantic, Deep-Sea Res., 16, 221–225, 1969.

Dittert, N., Baumann, K.-H., Bickert, T., Henrich, R., Huber, R., Kinkel, H., and Meggers, H.: Carbonate dissolution in the deep-sea: Methods, quantification and paleoceanographic application, in: Use of Proxies in Paleoceanography, edited by: Fischer, G. and Wefer, G., Springer, New York, 255–284, 1999.

Elderfield, H., Vautravers, M., and Cooper, M.: The relationship between shell size and Mg/Ca, Sr/Ca, $\delta^{18}O$, and $\delta^{13}C$ of species of planktonic foraminifera, Geochem. Geophys. Geosys., 3, doi:10.1029/2001GC000194, 2002.

Etourneau, J., Schneider, R., Blanz, T., and Martinez, P.: Intensification of the Walker and Hadley atmospheric circulations during the Pliocene-Pleistocene climate transition, Earth Planet. Sci. Lett., 297, 103–110, 2010.

Fairbanks, R. G., Sverdlove, M., Free, R., Wiebe, P., and Bé, W.: Vertical distribution and isotopic fractionation of living planktonic foraminifera from the Panama Basin, Nature, 298, 841–844, 1982.

Faul, K. L., Ravelo, A. C., and Delaney, M. L.: Reconstructions of upwelling, productivity, and photic zone depth in the eastern equatorial Pacific Ocean using planktonic foraminiferal stable isotopes and abundances, J. Foramin. Res., 30, doi:10.2113/0300110, 2000.

Fedorov, A. V. and Philander, S. G.: Is El Nino changing?, Science, 288, 1997–2002, 2000.

Fedorov, A. V., Pacanowski, R. C., Philander, S. G., and Boccaletti, G.: The effect of salinity on the wind-driven circulation and the thermal structure of the upper ocean, J. Phys. Oceanogr., 34, 1949–1966, 2004.

Fedorov, A. V., Dekens, P. S., McCarthy, M., Ravelo, A. C., deMenocal, P. B., Barriero, M., Pacanowski, R. C., and Philander, S. G.: The Pliocene paradox (mechanisms for a permanent El Niño), Science, 312, 1485–1489, 2006.

Ford, H. L., Ravelo, A. C., and Hovan, S.: A deep Eastern Equatorial Pacific thermocline during the early Pliocene warm period, Earth Planet. Sci. Lett., 355–356, 152–161, 2012.

Ford, H. L., Ravelo, A. C., Polissar, P. J.: Reduced El Niño–Southern Oscillation during the Last Glacial Maximum, Science, 347, 255–258, 2015.

Friedrich, O., Schiebel, R., Wilson, P. A., Weldeab, S., Beer, S. J., Cooper, M. J., and Fiebig, J.: Influence of test size, water depth, and ecology on Mg/Ca, Sr/Ca, $\delta^{18}O$ and $\delta^{13}C$ in nine modern species of planktic foraminifers, Earth Planet. Sci. Lett., 319, 133–145, 2012.

Greaves, M., Caillon, N., Rebaubier, H., Bartoli, G., Bohaty, S., Cacho, I., Clarke, L. J., Cooper, M., Daunt, C., Delaney, M., deMenocal, P., Dutton, A., Eggins, S., Elderfield, H., Garbe-Schoenberg, D., Goddard, E., Green, D., Groeneveld, J., Hastings, D., Hathorne, E., Kimoto, K., Klinkhammer, G., Labeyrie, L., Lea, D. W., Marchitto, T., Martinez-Boti, M. A., Mortyn, P. G., Ni, Y., Nuernberg, D., Paradis, G., Pena, L., Quinn, T., Rosenthal, Y., Russell, A., Sagawa, T., Sosdain, S., Stott, L., Tachikawa, K., Tappa, E., Thunell, R., Wilson, P. A.: Interlaboratory comparison study of calibration standards for foraminiferal Mg/Ca thermometry, Geochem. Geophys. Geosys., 9, Q08010, doi:08010.01029/02008GC001974, 2008.

Groeneveld, J., Steph, S., Tiedemann, R., Garbe-Schönberg, D., Nürnberg, D., and Sturm, A.: Pliocene mixed-layer oceanography for Site 1241, using combined Mg/Ca and $\delta^{18}O$ analyses of *Globigerinoides sacculifer*, in: Proc. ODP, Sci. Results, 202, College Station, TX (Ocean Drilling Program), edited by: Tiedemann, R., Mix, A. C., Richter, C., and Ruddiman, W. F., doi:10.2973/odp.proc.sr.202.209.2006, 2006.

Groeneveld, J., Hathorne, E.C., Steinke, S., DeBey, H., Mackensen, A., and Tiedemann, R.: Glacial induced closure of the Panamanian Gateway during Marine Isotope Stages (MIS) 95–100 (~2.5Ma), Earth Planet. Sci. Lett., 404, 296–306, 2014.

Hertzberg, J. E., Schmidt, M. W., Bianchi, T. S., Smith, R. W., Shields, M. R., and Marcantonio, F.: Comparison of eastern tropical Pacific TEX_{86} and *Globigerinoides ruber* Mg/Ca derived sea surface temperatures: Insights from the Holocene and Last Glacial Maximum, Earth Planet. Sci. Lett., 434, 320–332, 2016.

Jakob, K. A., Wilson, P. A., Bahr, A., Bolton, C. T., Pross, J., Fiebig, J., and Friedrich, O.: Plio-Pleistocene glacial-interglacial productivity changes in the eastern equatorial Pacific upwelling system, Paleoceanography, 31, 453–470, doi:410.1002/2015PA002899, 2016.

Jakob, K. A., Bolton, C. T., Wilson, P. A., Bahr, A., Pross, J., Fiebig, J., Kähler, K., Friedrich, O.: Glacial-interglacial changes in equatorial Pacific surface-water structure during the Plio-Pleistocene intensification of Northern Hemisphere Glaciation, Earth Planet. Sci. Lett., 463, 69–80, doi:10.1016/j.epsl.2017.1001.1028, 2017.

Jones, J. I.: Significance of distribution of planktonic foraminifers in the Equatorial Atlantic Undercurrent, Micropaleontology, 13, 489–501, 1967.

Jonkers, L., and Kučera, M.: Global analysis of seasonality in the shell flux of extant planktonic foraminifera. Biogeosciences, 12, 2207–2226, 2015.

Karas, C., Nürnberg, D., Gupta, A. K., Tiedemann, R., Mohan, K., and Bickert, T.: Mid-Pliocene climate change amplified by a switch in Indonesian subsurface throughflow. Nat.Geosci., 2, 434–438, 2009.

Kemle von Mücke, S. and Hemleben, C.: Foraminifera, in: South Atlantic Zooplankton, Vol. 1, edited by: Boltovskoy, D., Backhuys Publishers, Leiden, 43–74, 1999.

Koutavas, A. and Lynch-Stieglitz, J.: Glacial-interglacial dynamics of the eastern equatorial Pacific cold tongue-Intertropical Convergence Zone system reconstructed from oxygen isotope records, Paleoceanography, 18, doi:1010.1029/2003PA000894, 2003.

Kroopnick, P. M.: The distribution of ^{13}C of ΣCO_2 in the world oceans, Deep-Sea Res., 32, 57–84, 1985.

Lawrence, K. T., Liu, Z., and Herbert, T. D.: Evolution of the eastern tropical Pacific through Plio-Pleistocene glaciation, Science, 312, doi:10.1126/science.1120395, 2006.

Lee, S. Y. and Poulsen, C. J.: Tropical Pacific climate response to obliquity forcing in the Pleistocene, Paleoceanography, 20, PA4010, doi:4010.1029/2005PA001161, 2005.

Lin, H.-L., Peterson, L. C., Overpeck, J. T., Trumbore, S. E., and Murray, D. W.: Late Quaternary climate change from $\delta^{18}O$ records of multiple species of planktonic foraminifera: High-resolution records from the Anoxic Cariaco Basin, Venezuela, Paleoceanography, 12, 415–427, 1997.

Lisiecki, L. E. and Raymo, M. E.: A Pliocene-Pleistocene stack of 57 globally distributed benthic $\delta^{18}O$ records, Paleoceanography, 20, PA1003, doi:1010.1029/2004PA001071, 2005.

Locarnini, R. A., Mishonov, A. V., Antonov, J. I., Boyer, T. P., Garcia, H. E., Baranova, O. K., Zweng, M. M., Paver, C. R., Reagan, J. R., Johnson, D. R., Hamilton, M., and Seidov, D.: World Ocean Atlas 2013, Volume 1, Temperature, in: NOAA Atlas NESDIS 73, edited by: Levitus, S. and Mishonov, A., U. S. Government Printing Office, Washington, D. C., 40 pp, 2013.

Ma, H., Wu, L., and Li, Z.: Impact of freshening over the Southern Ocean on ENSO, Atmos. Sci. Lett., 14, 28–33, doi:10.1002/asl1002.1410, 2013.

Kim Jakob 6.4.18 12:16
Gelöscht: .

Martínez-Garcia et al., A., Rosell-Melé, A., McClymont, E. L., Gersonde, R., and Haug, G. H.: Subpolar link to the emergence of the modern equatorial Pacific cold tongue, Science, 328, 1550–1553, 2010.

Mayer, L., Pisias, N., and Janecek, T. et al.: Proc. ODP, Init. Repts., 138, College Station, TX, Ocean Drilling Program, 1992.

Mix, A. C., Pisias, N. G., Rugh, W., Wilson, J., Morey, A., and Hagelberg, T. K.: Benthic foraminifer stable isotope record from Site 849 (0–5 Ma): local and global climate changes, in: Proc. ODP, Sci. Results, 138, College Station, TX (Ocean Drilling Program), edited by: Pisias, N. G., Mayer, L. A., Janecek, T. R., Palmer-Julson, A., and van Adel, T. H., 371–412, 1995.

Mohtadi, M., Steinke, S., Groeneveld, J., Fink, H.G., Rixen, T., Hebbeln, D., Donner, B., and Herunadi, B.: Low-latitude control on seasonal and interannual changes in planktonic foraminiferal flux and shell geochemistry off south Java: A sediment trap study, Paleoceanography, 24, PA1201, doi:10.1029/2008PA001636, 2009.

Mudelsee, M. and Raymo, M. E.: Slow dynamics of the Northern Hemisphere Glaciation, Paleoceanography, 20, PA4022, doi:4010.1029/2005PA001153, 2005.

Naafs, B. D. A., Hefter, J., and Stein, R.: Millennial-scale ice rafting events and Hudson Strait Heinrich(-like) Events during the late Pliocene and Pleistocene: a review, Quaternary Sci. Rev., 80, 1–28, 2013.

Niebler, H.-S., Hubberten, H.-W., and Gersonde, R.: Oxygen isotope values of planktic foraminifera: A tool for the reconstruction of surface water stratification, in: Use of Proxies in Paleoceanography, edited by: Fischer, G. and Wefer, G., Springer, New York, 165–189, 1999.

Nürnberg, D., Böschen, T., Doering, K., Mollier-Vogel, E., Raddatz, J., and Schneider, R.: Sea surface and subsurface circulation dynamics off equatorial Peru during the last ~17 kyr, Paleoceanography, 30, 984–999, doi:910.1002/2014pa002706, 2015.

Pena, L. D., Calvo, E., Cacho, I., Eggins, S., and Pelejero, C.: Identification and removal of Mn-Mg-rich contaminant phases on foraminiferal tests: Implications for Mg/Ca past temperature reconstructions, Geochem. Geophys. Geosys., Q09P02, doi:10.1029/2005GC000930, 2005.

Pennington, J. T., Mahoney, K. L., Kuwahara, V. S., Kolber, D. D., Calienes, R., and Chavez, F. P.: Primary production in the eastern tropical Pacific: A review, Prog. Oceanogr., 69, 285–317, 2006.

Prell, W. L.: The stability of low-latitude sea-surface temperatures: an evaluation of the CLIMAP reconstruction with emphasis on the positive SST anomalies. Rep. TR 025, U.S. Dep. Energy, Washington, 60 pp., 1985.

Pusz, A. E., Thunell, R. C., and Miller, K. G. (2011). Deep water temperature, carbonate ion, and ice volume changes across the Eocene-Oligocene climate transition. Paleoceanography, 26, PA2205, doi:10.1029/2010PA001950, 2011.

Ravelo, A. C. and Hillaire-Marcel, C.: The use of oxygen and carbon isotopes of foraminifera in Paleoceanography, in: Proxies in Late Cenozoic Paleoceanography, edited by: Hillaire-Marcel, C. and De Vernal, A., Elsevier, Amsterdam, Oxford, 735–764, 2007.

Regenberg, M., Steph, S., Nürnberg, D., Tiedemann, R., and Garbe-Schönberg, D.: Calibrating Mg/Ca ratios of multiple planktonic foraminiferal species with δ^{18}O-calcification temperatures: Paleothermometry for the upper water column, Earth Planet. Sci. Lett., 278, 324–336, 2009.

Schlitzer, R.: Export production in the equatorial and north Pacific derived from dissolved oxygen, nutrient and carbon data, J. Oceanogr., 60, 53–62, 2004.

Schneider, B. and Schmittner, A.: Simulating the impact of the Panamanian seaway closure on ocean circulation, marine productivity and nutrient cycling, Earth Planet. Sci. Lett., 246, 367–380, 2006.

Sexton, P. F., and Norris, R. D.: Dispersal and biogeography of marine plankton: Long-distance dispersal of the foraminifer *Truncorotalia truncatulinoides*, Geology, 36, doi: 10.1130/G25232A, 2008.

Shackleton, N. J., Backman, J., Zimmerman, H., Kent, D. V., Hall, M., Roberts, D., Schnitker, D., Baldauf, J., Desprairies, A., and Homrighausen, R.: Oxygen isotope calibration of the onset of ice-rafting and history of glaciation in the North Atlantic region, Nature, 307, 620–623, 1984.

Spero, H. J., Mielke, K. M., Kalve, E. M., Lea, D. W., and Pak, D. K.: Multispecies approach to reconstructing eastern equatorial Pacific thermocline hydrography during the past 360 kyr, Paleoceanography, 18, doi:10.1029/2002PA000814, 2003.

Steph, S., Tiedemann, R., Groeneveld, J., Sturm, A., Nürnberg, D.: Pliocene changes in tropical east Pacific upper ocean stratification: Response to tropical gateways? Proc. ODP, Sci. Results, 202, College Station, TX (Ocean Drilling Program), edited by: Tiedemann, R. Mix, A. C., Richter, C., and Ruddiman, W. F., doi:10.2973/odp.proc.sr.202.211.2006, 2006a.

Steph, S., Tiedemann, R., Prange, M., Groeneveld, J., Nürnberg, D., Reuning, L., Schulz, M., and Haug, G. H.: Changes in Caribbean surface hydrography during the Pliocene shoaling of the Central American Seaway, Paleoceanography, 21, PA4221, doi:4210.1029/2004PA001092, 2006b.

Steph, S., Regenberg, M., Tiedemann, R., Mulitza, S., and Nürnberg, D.: Stable isotopes of planktonic foraminifera from tropical Atlantic/Caribbean core-tops: Implications for reconstructing upper ocean stratification, Mar. Micropaleontol., 71, 1–19, doi:10.1016/j.marmicro.2008.1012.1004, 2009.

Steph, S., Tiedemann, R., Prange, M., Groeneveld, J., Schulz, M., Timmermann, A., Nürnberg, D., Rühlemann, C., Saukel, C., and Haug, G. H.: Early Pliocene increase in thermohaline overturning: A precondition for the development of the modern equatorial Pacific cold tongue, Paleoceanography, 25, PA2202, doi:2210.1029/2008PA001645, 2010.

Takahashi, T., Sutherland, S. C., Wanninkhof, R., Sweeney, C., Feely, R. A., Chipman, D. W., Hales, B., Friederich, G., Chavez, F., Sabine, C., Watson, A., Bakker, D. C. E., Schuster, U., Metzl, N., Yoshikawa-Inoue, H., Ishii, M., Midorikawa, T., Nojiri, Y., Körtzinger, A., Steinhoff, T., Hoppema, M., Olafsson, J., Arnarson, T. S., Tilbrook, B., Johannessen, T., Olsen, A., Bellerby, R., Wong, C. S., Delille, B., Bates, N. R., de Baar, H. J. W.: Climatological mean and decadal change in surface ocean pCO_2, and net sea-air CO_2 flux over the global oceans, Deep-Sea Res. Pt II, 56, 554–577, 2009.

Kim Jakob 6.4.18 12:16
Gelöscht: 2006

Tedesco, K., Thunell, R., Astor, Y., and Muller-Karger, F.: The oxygen isotope composition of planktonic foraminifera from the Cariaco Basin, Venezuela: Seasonal and interannual variations, Mar. Micropaleontol., 62, 180–193, 2007.

Toggweiler, J. R. and Sarmiento, J. L.: Glacial to interglacial changes in atmospheric carbon dioxide: the critical role of ocean surface water in high latitudes, in: The carbon cycle and atmospheric CO_2: Natural variations Archean to present, edited by: Sundquist, E. T. and Broecker, W. S., Geoph. Monog. Series 32, American Geophysical Union, Washington, D. C., 163–184, 1985.

Tsuchiya, M., R. Lukas, A. R. Fine, E. Firing, and Lindstrom, E. J.: Source waters of the Pacific Equatorial Undercurrent, Prog. Oceanogr., 23, 101–147, 1989.

Wang, B., Wu, R., and Lukas, R.: Annual adjustment of the thermocline in the tropical Pacific Ocean, J. Climate, 13, 596–616, 2000.

Wang, L.: Isotopic signals in two morphotypes of *Globigerinoides ruber* (white) from the South China Sea: implications for monsoon climate change during the last glacial cycle, Palaeogeogr. Palaeoclim. Palaeoecol., 161, 381–394, 2000.

Wara, M. W., Ravelo, A. C., and Delaney, M. L.: Permanent El Niño-like conditions during the Pliocene warm period, Science, 309, 758–761, 2005.

Watkins, J. M., Mix, A. C., and Wilson, J.: Living planktic foraminifera in the central tropical Pacific Ocean: Articulating the equatorial “cold tongue” during La Niña, Mar. Micropaleontol., 33, 157–174, 1998.

Wejnert, K. E., Thunell, R. C., and Margarita Astor, Y.: Comparison of species-specific oxygen isotope paleotemperature equations: Sensitivity analysis using planktonic foraminifera from the Cariaco Basin, Venezuela, Mar. Micropaleontol., 101, 76–88, 2013.

Wilson, J., Abboud, S., and Beman, J. M.: Primary production, community respiration, and net community production along oxygen and nutrient gradients: Environmental controls and biogeochemical feedbacks within and across “Marine Lakes”, Front. Mar. Sci., 4, doi:10.3389/fmars.2017.00012, 2017.

Wyrtki, K.: An estimate of equatorial upwelling in the Pacific, J. Phys. Oceanogr., 11, 1205–1214, 1981.

Table 1: Compilation of the geochemical datasets from ODP Site 849 evaluated in this study. The number of samples indicates the total amount of samples processed (dried, weighed, washed) during each study, while the number of geochemical datapoints is somewhat lower depending on the availability of foraminiferal (*G. crassaformis* and *G. ruber*) material in each sample.

Foraminiferal species	Size fraction	Proxy	Interval	No. of samples (datapoints)	Reference
G. crassaformis (sinistral- and dextral-coiling)	315–400 µm	$\delta^{13}C$	74.17–67.78 mcd (~2.65–2.4 Ma; MIS G1–95)	229 (215)	Jakob et al. (2016)
			77.02–74.19 mcd (~2.75–2.65 Ma; MIS G7–G2)	145 (43)	this study
	315–400 µm	$\delta^{18}O$	77.02–67.78 mcd (~2.75–2.4 Ma; MIS G7–95)	374 (258)	this study
	315–400 µm	Mg/Ca	77.02–67.78 mcd (~2.75–2.4 Ma; MIS G7–95)	374 (247)	this study
G. ruber (white, sensu stricto)	250–315 µm	$\delta^{13}C$	74.17–67.78 mcd (~2.65–2.4 Ma; MIS G1–95)	229 (225)	Jakob et al. (2016)
			77.02–74.19 mcd (~2.75–2.65 Ma; MIS G7–G2)	145 (137)	this study
	250–315 µm	$\delta^{18}O$	77.02–67.78 mcd (~2.75–2.4 Ma; MIS G7–95)	374 (362)	Jakob et al. (2017)
	200–250 µm	Mg/Ca	77.02–67.78 mcd (~2.75–2.4 Ma; MIS G7–95)	374 (316)	Jakob et al. (2017)

Kim Jakob 6.4.18 12:16
Gelöscht: . ... [7]

Kim Jakob 6.4.18 12:16
Formatierte Tabelle

Kim Jakob 6.4.18 12:16
Eingefügte Zellen

Kim Jakob 6.4.18 12:16
Formatiert: Links

Kim Jakob 6.4.18 12:16
Zusammengeführte Zellen

Kim Jakob 6.4.18 12:16
Zusammengeführte Zellen

Kim Jakob 6.4.18 12:16
Zusammengeführte Zellen

Kim Jakob 6.4.18 12:16
Formatiert: Links

Kim Jakob 6.4.18 12:16
Zusammengeführte Zellen

Kim Jakob 6.4.18 12:16
Zusammengeführte Zellen

Kim Jakob 6.4.18 12:16
Zusammengeführte Zellen

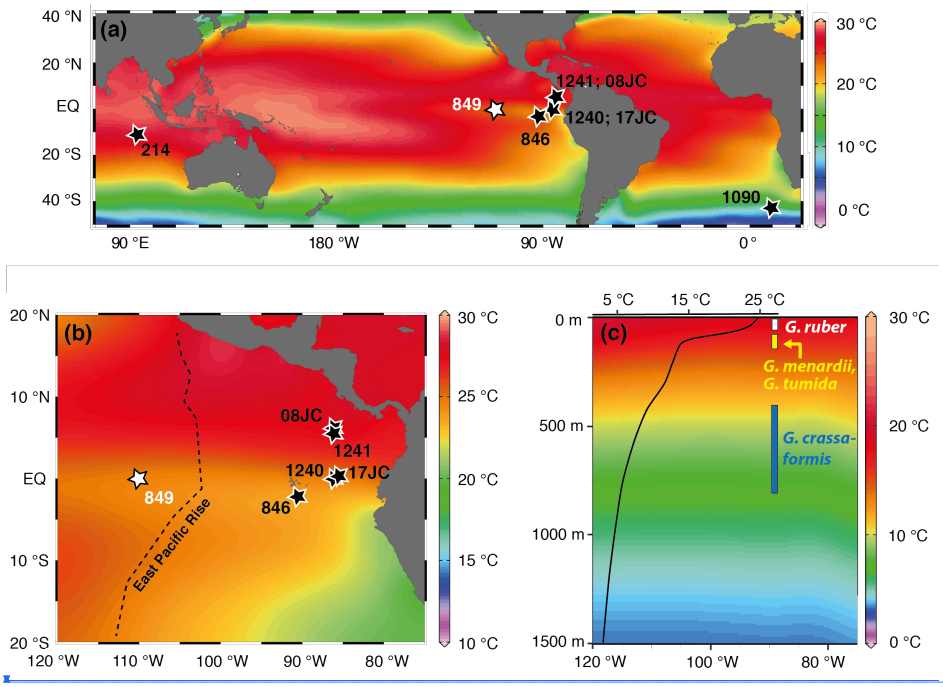

Figure 1: Location of study area and present-day temperature profile at studied site. (a) Map indicating the location of the study site (ODP Site 849; white) and other sites mentioned in the text (black). (b) Map showing the location of Site 849 in the EEP "cold tongue" (white) and other east Pacific sites mentioned in the text (black). Colors in (a) and (b) denote mean annual surface-water temperatures. (c) Mean annual temperature profile for Site 849 showing the position of the thermocline. Calcification depths of foraminiferal species analyzed in this study are indicated by white (*G. ruber*), yellow (*G. menardii* and *G. tumida*) and blue (*G. crassaformis*) bars (because the calcification depth of *G. crassaformis* in the EEP remains unclear, we here show its calcification depth range identified for the [sub-]tropical Atlantic and the Caribbean Sea; see Section 3 for details). Maps are after World Ocean Atlas (Locarnini et al., 2013).

Kim Jakob 6.4.18 12:16
Gelöscht: . ... [8]

Unknown
Formatiert: Schriftart:Fett

Kim Jakob 6.4.18 12:16
Gelöscht: within the Eastern Equatorial Pacific

Kim Jakob 6.4.18 12:16
Gelöscht: ODP

Kim Jakob 6.4.18 12:16
Gelöscht: "

Kim Jakob 6.4.18 12:16
Gelöscht: ".

Kim Jakob 6.4.18 12:16
Gelöscht: b

Kim Jakob 6.4.18 12:16
Gelöscht: Sect.

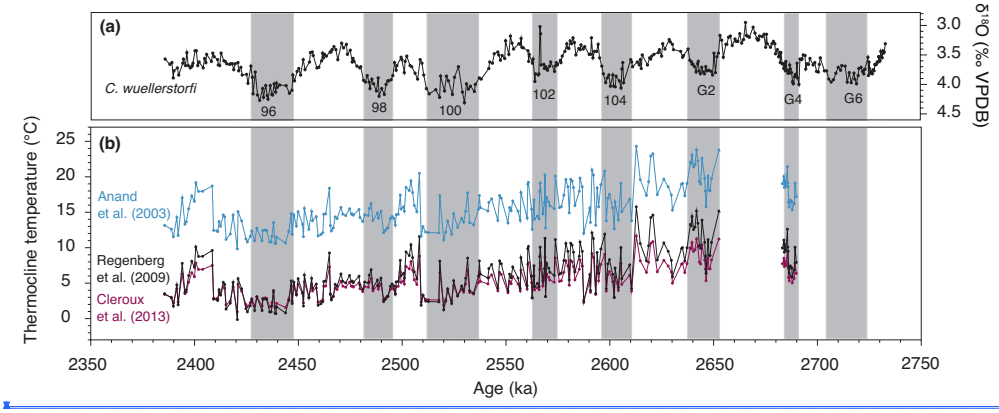

Figure 2: Species-specific conversions of Mg/Ca ratios to temperature for *G. crassaformis*. (a) Benthic foraminiferal (*C. wuellerstorfi*) $\delta^{18}O$ stratigraphy (Jakob et al., 2017). (b) Comparison of the different species-specific Mg/Ca-to-temperature conversions of Cléroux et al. (2013, red), Regenberg et al. (2009, black) and Anand et al. (2003, blue) applied to *G. crassaformis* Mg/Ca values from Site 849 for ~2.75 to 2.4 Ma. Gaps in the dataset for 2.68–2.65 Ma (MIS G3) and 2.73–2.69 Ma (MIS G7–G5) are due to a lack of *G. crassaformis* specimens in the investigated (315–400 µm) size fraction. Grey bars highlight glacial periods.

Kim Jakob 6.4.18 12:16
Gelöscht: ... [9]

Unknown
Formatiert: Schriftart:Fett, Kursiv

Unknown
Formatiert: Schriftart:Fett, Kursiv

Kim Jakob 6.4.18 12:16
Gelöscht:

Kim Jakob 6.4.18 12:16
Gelöscht:

Kim Jakob 6.4.18 12:16
Gelöscht:) (

Kim Jakob 6.4.18 12:16
Gelöscht:) (

Kim Jakob 6.4.18 12:16
Gelöscht:) (

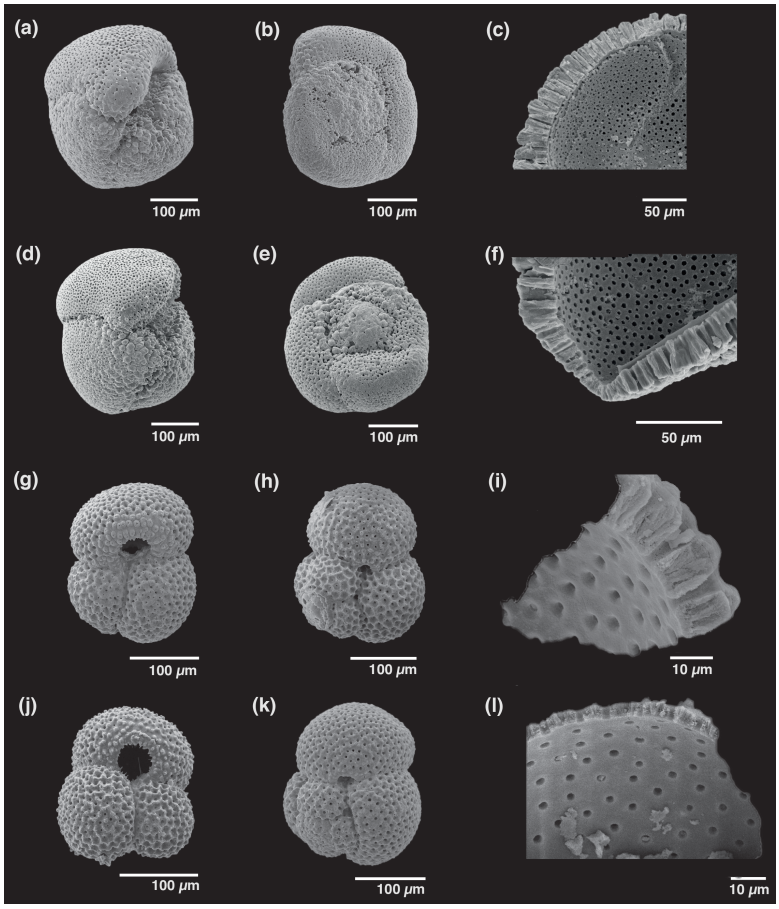

Figure 3: Scanning Electron Micrographs of *Globorotalia crassaformis* and *Globigerinoides ruber* from Site 849. Both glacial (a–c, g–i) and interglacial (d–f, j–l) foraminiferal tests are well preserved, allowing for the acquisition of reliable geochemical data.

Kim Jakob 6.4.18 12:16
Gelöscht: ODP

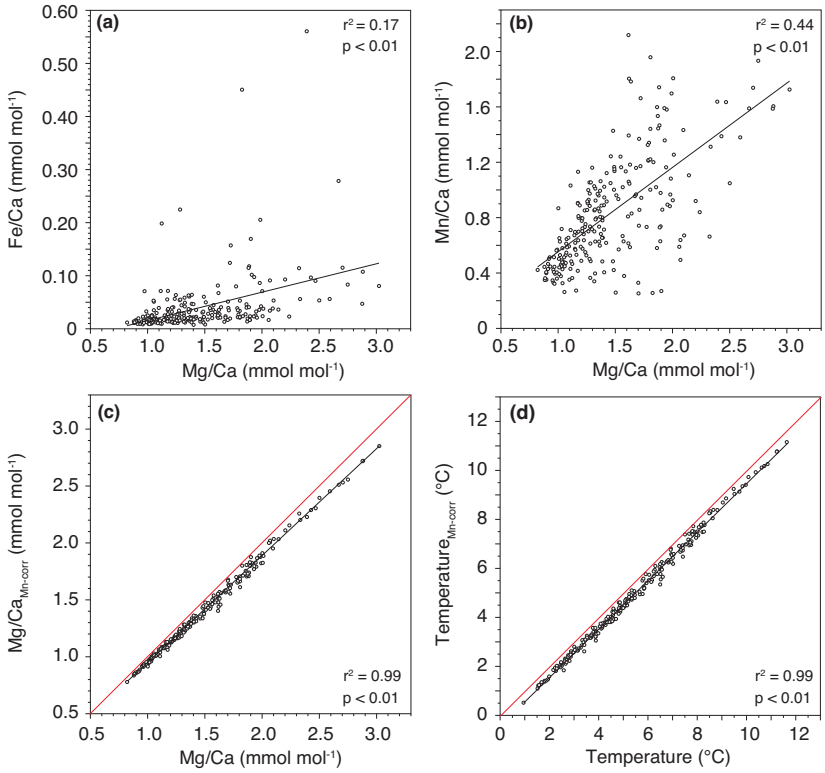

Figure 4: Evaluation of potential contamination on Mg/Ca ratios in *G. crassaformis*. (a) Cross plot between measured Mg/Ca and Fe/Ca ratios. (b) Cross plot between measured Mg/Ca and Mn/Ca ratios. (c) Cross plot between measured Mg/Ca and Mg/Ca ratios corrected for Mn-bearing overgrowths (using the assumption of an unrealistically high Mg/Mn ratio of 1) in comparison to uncontaminated samples (red line). (d) Cross plot between temperatures calculated from measured Mg/Ca and Mg/Ca ratios corrected for Mn-bearing overgrowths (using the assumption of an unrealistically high Mg/Mn ratio of 1) in comparison to uncontaminated samples (red line) (see Section 5.2 for details).

Kim Jakob 6.4.18 12:16

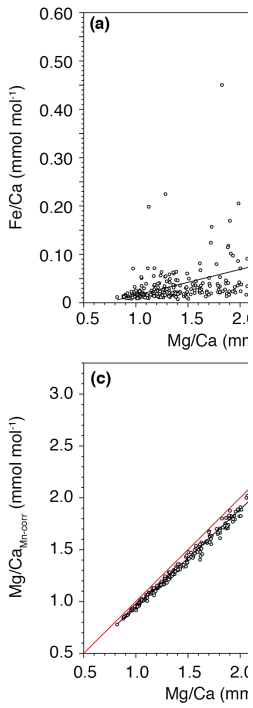

Gelöscht:

Unknown

Formatiert: Schriftart:Fett

Kim Jakob 6.4.18 12:16

Gelöscht: Sect.

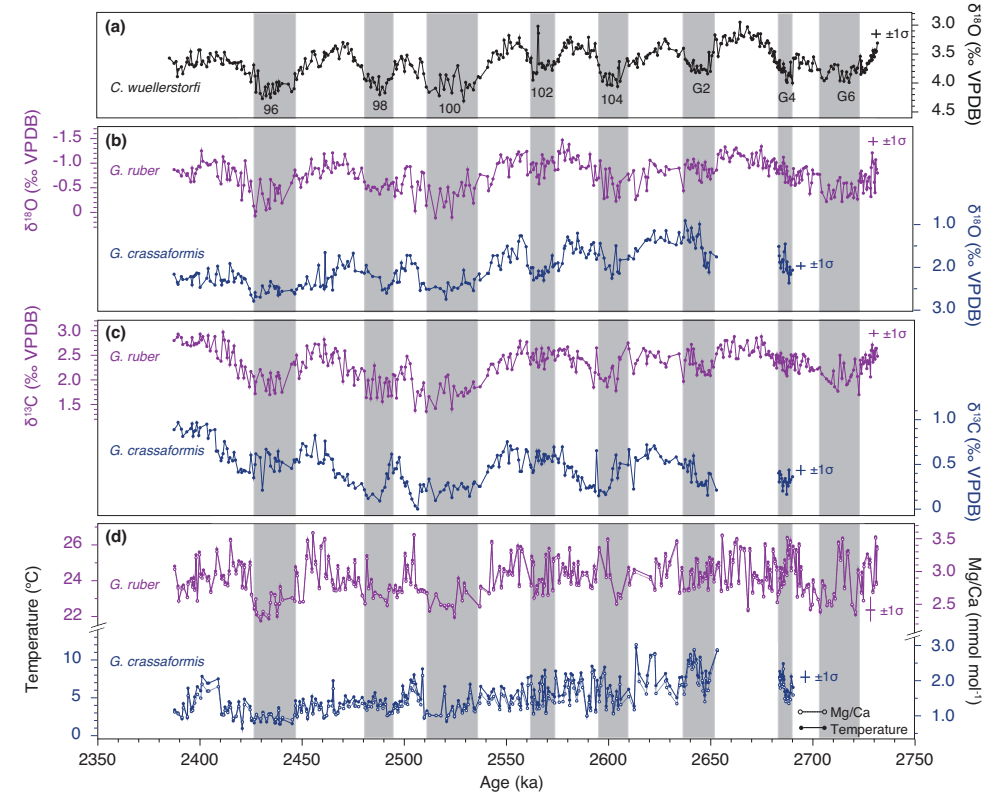

Figure 5: Planktic foraminiferal proxy records from ODP Site 849 for MIS G7–95 (~2.75–2.4 Ma). (a) Benthic foraminiferal (*C. wuellerstorfi*) $\delta^{18}O$ stratigraphy (Jakob et al., 2017). (b) $\delta^{18}O$ data of *G. ruber* (purple; Jakob et al., 2017) and *G. crassaformis* (blue; this study). (c) $\delta^{13}C$ data of *G. ruber* (purple; Jakob et al., 2016, this study) and *G. crassaformis* (blue; Jakob et al., 2016, this study). (d) Mg/Ca (dashed line, open dots) and temperature (solid line, filled dotes) data of *G. ruber* (purple; Jakob et al., 2017) and *G. crassaformis* (blue; this study). Gaps in the *G. crassaformis* dataset for 2.68–2.65 Ma (MIS G3) and 2.73–2.69 Ma (MIS G7–G5) are due to a lack of *G. crassaformis* specimens in the investigated (315–400 µm) size fraction. Horizontal and vertical bars indicate the 1σ standard deviation associated with the age model and the individual proxy records, respectively. Grey bars highlight glacial periods.

Kim Jakob 6.4.18 12:16
Gelöscht:

Kim Jakob 6.4.18 12:16
Gelöscht: . […, 2017])… and *G. crassafo* ... [10]

Kim Jakob 6.4.18 12:16
Formatiert ... [11]

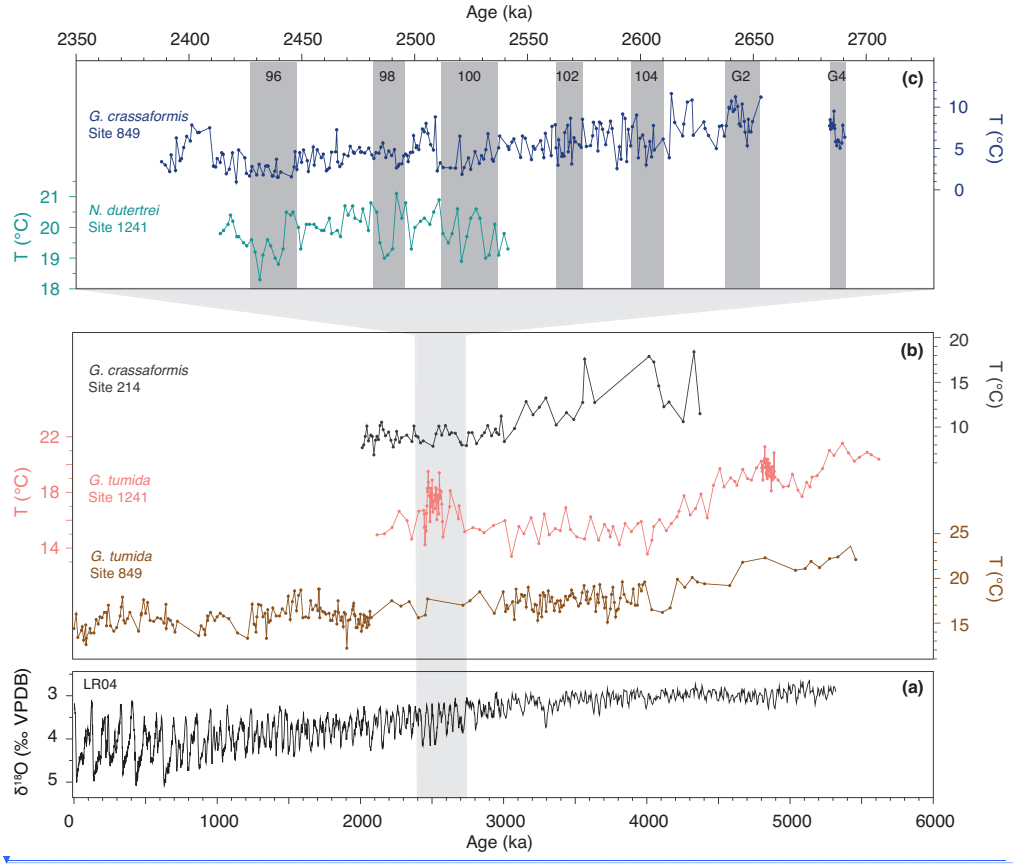

Kim Jakob 6.4.18 12:16

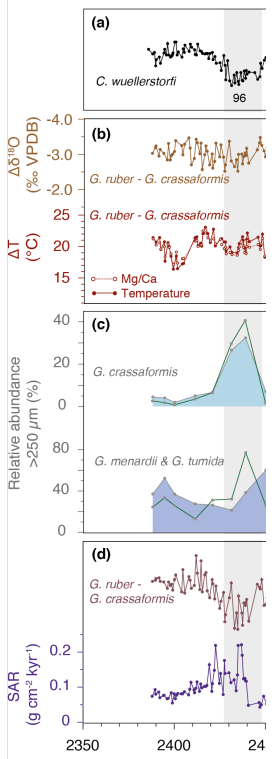

Gelöscht: ... [12]

Figure 6: Comparison of selected thermocline-temperature records from the tropical Pacific for the past ~6 Myr (bottom) and the ~2.75–2.4 Ma interval (top). (a) Benthic oxygen isotope record (LR04 stack; Lisiecki and Raymo, 2005). (b) Low-resolution Mg/Ca-based temperature records of thermocline-dwelling species from Site 214 (grey; Karas et al., 2009), Site 1241 (pink; Steph et al., 2006a) and Site 849 (brown; Ford et al., 2012). Light grey shading in a and b marks the investigated time period of this study. (c) High-resolution Mg/Ca-based temperature records of thermocline-dwelling species from Site 849 (blue; this study) and Site 1241 (cyan; Groeneveld et al., 2014). Grey bars highlight glacial periods.

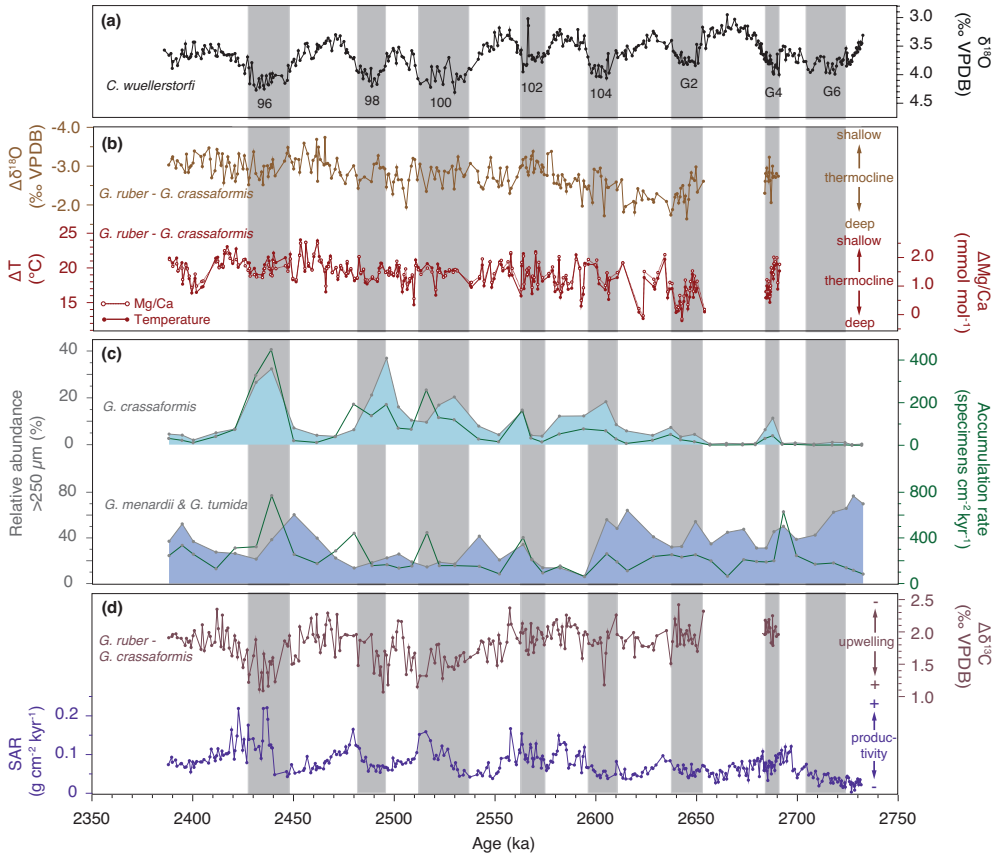

Figure 7: Compilation of planktic foraminiferal, faunal and sedimentary proxy records from ODP Site 849 for MIS G7–95 (~2.75–2.4 Ma). (a) Benthic foraminiferal (*C. wuellerstorfi*) $\delta^{18}O$ stratigraphy (Jakob et al., 2017). (b) $\delta^{18}O$ (brown; this study) and Mg/Ca (red dashed line with open dots; this study) and temperature (red; this study) gradients between the surface-dwelling species *G. ruber* and the thermocline-dwelling species *G. crassaformis* as a proxy for relative thermocline depth. (c) Relative abundances of *G. crassaformis* (light blue; this study) and *G. menardii* and *G. tumida* (dark blue; this study) together with their mass-accumulation rates (green; this study). (d) $\delta^{13}C$ gradient between *G. ruber* and *G. crassaformis* as an indicator for upwelling strength (purple; Jakob et al., 2016, this study) together with sand-accumulation rates (SAR) as an indicator for primary productivity (Jakob et al., 2016, this study). Gaps in the $\delta^{18}O$, $\delta^{13}C$ and Mg/Ca gradients for 2.68–2.65 Ma (MIS G3) and 2.73–2.69 Ma (MIS G7–G5) are due to a lack of *G. crassaformis* specimens in the investigated (315–400 µm) size fraction. Grey bars highlight glacial periods.

Kim Jakob 6.4.18 12:16
Gelöscht: . [

Kim Jakob 6.4.18 12:16
Gelöscht:],

Kim Jakob 6.4.18 12:16
Gelöscht: . [

Kim Jakob 6.4.18 12:16
Gelöscht:],

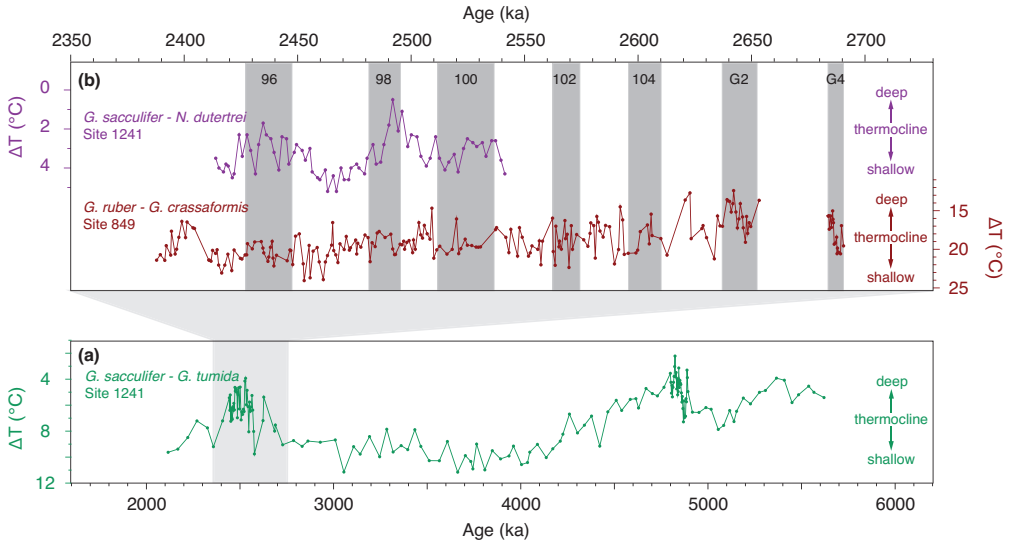

Figure 8: Comparison of selected thermocline-depth proxy records from the east Pacific for the ~6–2 Ma (bottom) and the ~2.75–2.4 Ma (top) intervals. (a) Low-resolution surface-to-thermocline temperature gradient from Site 1241 (green; Groeneveld et al., 2006; Steph et al., 2006a) reflecting relative thermocline depth changes. Light grey shading marks the investigated time period of this study. (b) High-resolution surface-to-thermocline temperature gradients from Site 849 (red; this study) and Site 1241 (purple; Groeneveld et al., 2014) indicative of relative thermocline depth changes. Grey bars highlight glacial periods.